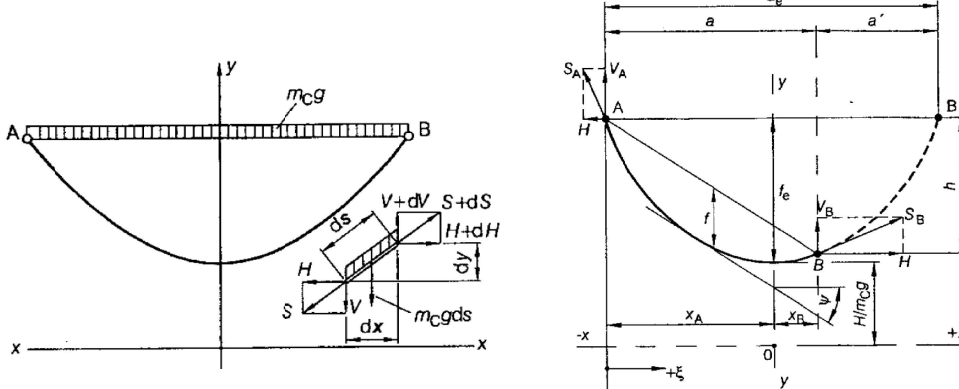


Chapter 3 Structural Considerations of Overhead Line

Transmission lines comprises overhead lines and cables. Although overhead lines are often tripped with **transient fault** due to vegetation and lightning, it does have its advantages on less thermal rating concerns and low construction cost. Yet, the major considerations for OHL applications other than faults are mostly structural, including **corona** and **mechanical fatigue** due to oscillations with wind, **cascade failure** of tower structure due to rusting, lack of **clearance** due to **thermal annealing** of overloading OHL, and **foundation failure** due to surrounding groundworks. Its auxiliaries including V-rod, spark gap, insulators, marker balls and dampers can also fail and fall.

3.1 Sag and Tension – Equation of Catenary



In case of stranded conductor used for OHL, it may be assumed that uniform **dimension** and **mechanical characteristics** at least between two adjacent support. To determine the sagging curve $y = f(x)$, the equilibrium conditions are established for the force acting at the differential element with infinitesimal length ds . For vertical force balance,

$$m_{cg} ds = V + dV - V \quad (3.1)$$

and because of

$$ds = \sqrt{dx^2 + dy^2} = dx \sqrt{1 + \left(\frac{dy}{dx}\right)^2} \quad (3.2)$$

it results in

$$\frac{dV}{dx} = m_{cg} \sqrt{1 + \left(\frac{dy}{dx}\right)^2} \quad (3.3)$$

The balance of forces in horizontal direction yields

$$H + dH - H = 0 \rightarrow dH = 0 \quad (3.4)$$

The horizontal component H of the conductor tensile force does not change along the conductor sagging curve. The balance of moments around the center of gravity of the conductor element results in

$$Hdy = Vdx \rightarrow V = H \frac{dy}{dx} \quad (3.5)$$

Differentiate (3.5) and substitute into (3.3),

$$\frac{d^2y}{dx^2} = \frac{m_{cg}}{H} \sqrt{1 + \left(\frac{dy}{dx}\right)^2} \quad (3.6)$$

It is noted that the conductor tensile stress $\sigma = H/A$ was not introduced into (3.6) as it applies exactly also for composite conductors for which the ratio H/A forming the equivalent tensile stress does not represent a measurable physical quantities.

Rearrange and Integrate,

$$\frac{\frac{d^2y}{dx^2} dy}{\sqrt{1 + \left(\frac{dy}{dx}\right)^2}} dx = \frac{m_{cg}}{H} \frac{dy}{dx} dx \rightarrow \sqrt{1 + \left(\frac{dy}{dx}\right)^2} = m_{cg} y \frac{C}{H} = \frac{m_{cg}(y - y_0)}{H} \quad (3.7)$$

Solving,

$$\frac{dy}{dx} = \sqrt{\left[\frac{m_{cg}(y - y_0)}{H}\right]^2 - 1} \rightarrow y = \frac{H}{m_{cg}} \left\{ \cosh \frac{m_{cg}}{H} (x - x_0) + C_0 \right\} \quad (3.8)$$

Equation (3.8) shows that a conductor sagged between the point A and B will take the shape of hyperbolic shape. Yet, Equation (3.8) is not well suited for practical use. Hence, the origin of the coordinate system is chosen such that the vertex of sagging line has the coordinates $x = 0, y = H/m_{cg}$. Using this coordinate, the conductor can be represented by

$$y = \frac{H}{m_{cg}} \cosh \frac{m_{cg}}{H} x \quad (3.9)$$

If A and B are NOT at the same height, as illustrated in the figure, the sag of a given point at the conductor related to the connection line of the point A and B follows to be

$$f = \frac{h}{a}(x - x_A) + \frac{H}{m_{cg}} \left[\cosh \frac{m_{cg}}{H} x_A - \cosh \frac{m_{cg}}{H} x \right] \quad (3.10)$$

where x_A designates the **abscissa** of the fixing point A, which has still to be determined. In particular, the sag of the vertex S is obtained from (3.10) for $x = 0$ is

$$f_0 = \frac{H}{m_{cg}} \left[\cosh \frac{m_{cg}}{H} x_A - 1 \right] - \frac{h}{a} x_A \quad (3.11)$$

In general, the span length a , the difference in height h of the attachment points, the mass per unit length and horizontal tensile force are given for an overhead line span, but not the position of vertex expressed by the coordinate x_A . The sag will be zero for point A and B. From (3.10), it is obtained with $x = x_B$ and $x_B - x_A = a$

$$h = \frac{H}{m_C g} \left[\cosh \frac{m_C g}{H} x_B - \cosh \frac{m_C g}{H} x_A \right] \quad (3.12)$$

With the addition formulae for hyperbolic function,

$$h = \frac{2H}{m_C g} \sinh \frac{m_C g(x_A + x_B)}{2H} \sinh \frac{m_C g(x_B - x_A)}{2H} \quad (3.13)$$

The equation (3.13) can be solved explicitly regarding the variable x_A if the conductor length between the suspension point A and B is introduced.

$$L = \int_{x_A}^{x_B} \sqrt{1 + \left(\frac{dy}{dx} \right)^2} dx = \int_{x_A}^{x_B} \sqrt{1 + \sinh^2 \frac{m_C g x}{H}} dx = \int_{x_A}^{x_B} \cosh \frac{m_C g x}{H} dx \quad (3.14)$$

It is obtained that

$$L = \frac{H}{m_C g} \left[\sinh \frac{m_C g x_B}{H} - \sinh \frac{m_C g x_A}{H} \right] = \frac{2H}{m_C g} \cosh \frac{m_C g(x_A + x_B)}{2H} \sinh \frac{m_C g(x_B - x_A)}{2H} \quad (3.15)$$

With $\cosh^2 x - \sinh^2 x = 1$ the conductor length is obtained using $x_B - x_A = a$

$$L = \sqrt{h^2 + \left[\frac{2H}{m_C g} \sinh \left(\frac{m_C g a}{2H} \right) \right]^2} \quad (3.16)$$

Solving with respect to x_A ,

$$x_A = \frac{H}{m_C g} \ln \left[\frac{H}{m_C g(L-h)} \left(1 - \exp \left(-\frac{m_C g a}{H} \right) \right) \right] \quad (3.17)$$

If both attachment points A and B are situated at the same level, the vertex will be in the center line of the span because of symmetry. The maximum sag can be obtained for $x = 0$:

$$f = \frac{H}{m_C g} \left[\cosh \frac{m_C g a}{2H} - \cosh \frac{m_C g x}{H} \right] \rightarrow f_{Max} = \frac{H}{m_C g} \left[\cosh \frac{m_C g a}{2H} - 1 \right] \quad (3.18)$$

With (3.5) and (3.9), the vertical component $V(x)$ of the conductor tensile force is obtained with

$$V = H \sinh \frac{m_C g}{H} x \quad (3.19)$$

This force acts against the gravitation in case of a positive sign. The support forces at the point A and B follow using $G = -V$:

$$G_A = -H \sinh \left(\frac{m_C g}{H} x_A \right), \quad G_B = H \sinh \left(\frac{m_C g(a+x_A)}{H} \right) \quad (3.20)$$

The total tensile force is equal to the horizontal force at the vertex of the sagging curve and increases towards the suspension point according to

$$S = \sqrt{H^2 + V^2} = H \sqrt{1 + \sinh^2 \left(\frac{m_C g}{H} x \right)} = H \cosh \left(m_C g \frac{x}{H} \right) \quad (3.21)$$

The mean value of conductor tensile force can be calculated from

$$\bar{S} = \frac{1}{a} \int_{x_A}^{x_B} S dx = \frac{H}{a} \int_{x_A}^{x_B} \cosh \frac{m_C g}{H} x dx = \frac{H}{a} L \underbrace{\cosh}_{L}$$

With sufficient accuracy, it is assumed for many practical application that the gradient of the tangent to sagging curve is small, i.e.

$$\frac{d^2 y}{dx^2} = \frac{m_C g}{H} \approx 0 \quad (3.22)$$

Neglecting the term, by carrying out two integration,

$$\frac{d^2 y}{dx^2} = \frac{m_C g}{H} \rightarrow y = \frac{m_C g}{2H} x^2 + C_1 x + C_2 \quad (3.23)$$

Putting the origin of the coordinate at the vertex, yield $C_1 = C_2 = 0$, i.e.

$$y = \frac{m_C g}{2H} x^2 \quad (3.24)$$

It is named as **parabolic estimation**.

The sag of a given point of the conductor compared to the connection line of the attachment points A and B yields

$$f = \frac{h}{a} (x - x_A) + \frac{m_C g}{2H} (x_A^2 - x^2) \quad (3.25)$$

Moving the origin of the coordinate system to the attachment point A yields the maximum value

$$f = \frac{m_C g a^2}{2H} \left(\frac{\xi}{a} - \frac{\xi^2}{a^2} \right) \rightarrow f_{Max} = \frac{m_C g a^2}{8H} \quad (3.26)$$

where $\xi = x + x_A$.

Compare (3.18) with (3.26), developing $\cosh(x)$ into a Taylor Series results in

Exact Solution:

$$f_{Max} = \frac{H}{m_C g} \left[\cosh \frac{m_C g a}{2H} - 1 \right] \quad (3.18)$$

Simplified Solution:

$$f_{Max} = \frac{m_C g a^2}{8H} \quad (3.26)$$

Taylor Series Expansion:

$$f_{Max} = \frac{m_C g a^2}{8H} + \frac{(m_C g)^3 a^4}{384 H^3} + \frac{(m_C g)^5 a^6}{46080 H^5} + \dots \quad (3.27)$$

Sag and Tension Calculation – Same Level:

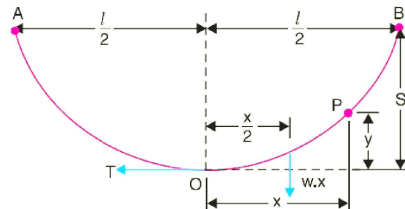
Suppose, AOB is the conductor. A and B are points of supports. Point O is the lowest point and the midpoint.

Let, L = length of the span, i.e. AB, w = the weight per unit length of the conductor, T = the tension in the conductor
Take Moment about O:

$$Ty = wx \frac{x}{2} \rightarrow y = \frac{wx^3}{2T} \quad (3.28)$$

Maximum Sag:

$$S \left(\frac{L}{2} \right) = \frac{w^2 L^3}{8T} \quad (3.29)$$



Sag and Tension Calculation – Different Level:

Suppose AOB is the conductor that has point O as the lowest point.

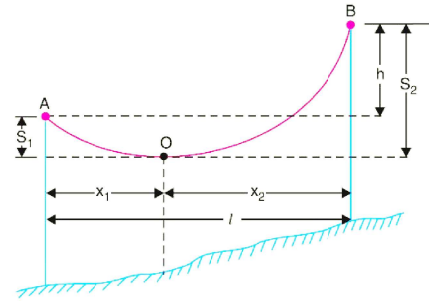
Similarly,

$$S_1 = \frac{wx_1^2}{8T}, \quad S_2 = \frac{wx_2^2}{8T}, \quad x_1 + x_2 = L \quad (3.30)$$

$$S_1 - S_2 = \frac{w}{8T} (x_1^2 - x_2^2) = \frac{wL}{8T} (x_1 - x_2) \rightarrow h = \frac{wL}{8T} (x_1 - x_2) \quad (3.31)$$

Solving (3.30) and (3.31),

$$x_1 = \frac{L}{2} - \frac{Th}{wL}, \quad x_2 = \frac{L}{2} + \frac{Th}{wL} \quad (3.32)$$



Sag and Tension Calculation – With Effect of Wind and Ice Load

w = weight per unit length of conductor

w_i = weight of ice per unit length = density of ice × volume per unit length = $\rho \times \pi t(d+t)$

w_w = wind force per unit length

= wind pressure per unit area × projected area per unit length

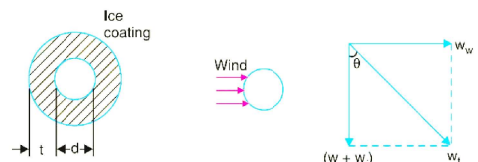
= wind pressure × [d + 2t]

Given that total load:

$$w_t = \sqrt{(w + w_i)^2 + (w_w)^2} \quad (3.33)$$

with slant sag and vertical sag:

$$S_s = \frac{w_t L^2}{8T}, \quad S = S_s \cos \theta \quad (3.34)$$



Example 1:

An overhead line has a span of 150m between level support. The conductor has a cross-sectional area of 2cm². The tension in the conductor is 2000kN. If the specific gravity of the conductor material is 9.9g/cm³ and wind pressure is 1.5 kg/m length. Calculate the sag.

Example 2:

An overhead line conductor having a parabolic configuration weight 1.925 kg/m. The area of cross section of the conductor is 2.2 cm² and the ultimate strength is 8000kg/cm². The support are 600 m apart and having 15 m difference of levels. Assume that the ice load is 1kg/m and there is no wind pressure. With factor of safety = 5, calculate the sag from the taller supports.

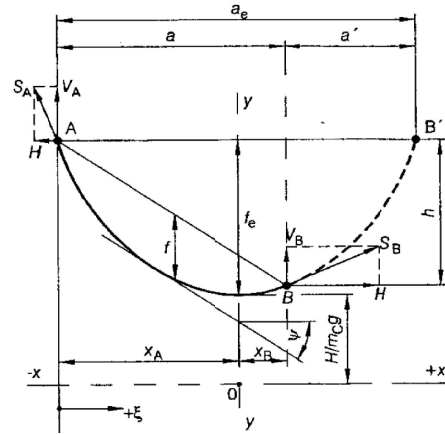
The equation (3.10) applies as well for the sag in a span with difference height levels at both ends. In many cases it is advantageous for calculating to expand the span ideally, such that the attachment points have the same level in the complementary span in order to be able to apply the simpler relations for this case. Therefore the complementary span length a_e in the expanded span can be calculated. With $a_e = 2|x_A|$,

$$a_e = \frac{2H}{m_C g} \ln \frac{\left(1 - \exp\left(-\frac{m_C g a}{H}\right)\right)}{L - h} \quad (3.28)$$

Using the parabola for the sagging line, it is obtained from (3.25) that

$$f \Big|_{x_B} = \frac{h}{a} (x_B - x_A) + \frac{m_C g}{2H} (x_A^2 - x_B^2) = 0 \quad (3.25)$$

$$x_A = -\frac{a}{2} + \frac{H-h}{m_C g a} \rightarrow a_e = 2x_A = a + \frac{2Hh}{m_C g a} \quad (3.29)$$



If (3.18) is used for sag in complementary span (3.21), it applies for the conductor tensile force at the attachment point A with

$$\cosh \frac{m_C g a_e}{2H} = \frac{f_e m_C g}{H} + 1$$

$$S_A = H + f_e \cdot m_C g \quad (3.30)$$

and attachment B accordingly,

$$S_B = H + (f_e - h) \cdot m_C g \quad (3.31)$$

If the temperature or loading of a conductor can affect the conductor length, the length of conductor in condition 2 can be represented in function of characteristics in condition 1, i.e.

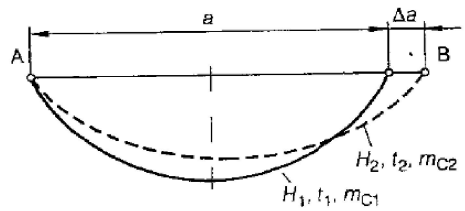
$$L_2 = L_1 (1 + e_{th}) (1 + e_{el}) \quad (3.32)$$

where e_{th} and e_{el} are the thermal and elastic expansion, respectively. With the relation that

$$e_{th} = \varepsilon_t \Delta T \quad e_{el} = \frac{\Delta S}{EA}$$

The expanded length can be further represented by

$$L_2 = L_1 (1 + \varepsilon_t (T_2 - T_1)) (1 + \frac{S_2 - S_1}{EA}) \quad (3.33)$$



With parabolic estimation,

$$L = a \left(1 + \frac{(m_C g)^2 a^2}{24H^2} \right) \quad (3.34)$$

With force S_1 and S_2 obtained from (3.21)

$$\bar{S}_1 = H_1 \frac{L_1}{a} \quad \bar{S}_2 = H_2 \frac{L_2}{a} \quad (3.35)$$

With acceptable accuracy, it applies $(S_2 - S_1) \sim (H_2 - H_1)$. Inserting these terms in (3.33) yields

$$L_2 = L_1 (1 + \varepsilon_t (T_2 - T_1)) (1 + \frac{S_2 - S_1}{EA}) \quad (3.36)$$

$$a \left(1 + \frac{(m_C g)^2 a^2}{24H_2^2} \right) = a \left(1 + \frac{(m_C g)^2 a^2}{24H_1^2} \right) (1 + \varepsilon_t (T_2 - T_1)) \left(1 + \frac{H_2 - H_1}{EA} \right) \approx a + a\varepsilon_t (T_2 - T_1) + a \frac{H_2 - H_1}{EA} + \frac{a^3 (m_C g)^2}{24H_1^2} \quad (3.37)$$

Simplifying, the **conductor state change equation** is obtained.

$$H_2^2 [H_2 - H_1 + \frac{EA(a m_C g)^2}{24H_1^2} + EA \varepsilon_t (T_2 - T_1)] = \frac{EA(a m_C g)^2}{24} \quad (3.38)$$

In equation (3.37), the conductor tensile forces is the unknown variable. Equation (3.37) is, therefore, correct for all conductor types, whether being single-material or composite conductors. The equivalent tensile stress $\sigma = H/A$ can be introduced and leads to

$$\sigma_2^2 [\sigma_2 - \sigma_1 + \frac{E(a m_C g)^2}{24H_1^2 A^2} + E \varepsilon_t (T_2 - T_1)] = \frac{E(a m_C g)^2}{24A^2} \quad (3.39)$$

The tensile stress can be measured physically only at single material conductors. The conductor state change equation is an algebraic equation of the 3rd degree which can be practically solved by numeric procedures available on calculators. If the span length is increased by the value Δa , e.g. by swinging of a suspension set, the characteristics of the conductor state will vary as well. As

$$L_2 = a + \Delta a + (a + \Delta a)^3 \frac{(m_C g)^2}{24H_2^2} \approx a + \Delta a + a^3 \frac{(m_C g)^2}{24H_2^2} \quad (3.40)$$

with the mentioned approximation, it is obtained from (3.36) that

$$H_2^2 [H_2 - H_1 + \frac{EA(a m_C g)^2}{24H_1^2} + EA \varepsilon_t (T_2 - T_1) - \frac{EA \Delta a}{a}] = \frac{EA(a m_C g)^2}{24} \quad (3.41)$$

The conductor state change equation (3.38) or (3.39) can be applied to a tensioning section of an overhead power line with n spans, assuming the conductor force H_i and the loading m_{Ci} are equal in all spans. This approximation is more precise than the assumption of rigid attachment points in each span. In a tensioning section, it applies to the total conductor length L_1 or L_2 .

$$L_{i,1,2} = \sum_{i=1}^n \left[a_i + a_i^3 \frac{(m_{c1,2}g)^2}{24H_{i,2}^2} \right] \quad (3.42)$$

When neglecting again the terms which are small by a higher order of magnitude, it is obtained from (3.36) that

$$H_2^2 [H_2 - H_1 + \frac{EA(m_{c1}g)^2}{24H_1^2} \left(\frac{\sum_{i=1}^n a_i^3}{\sum_{i=1}^n a_i} \right) + EA \varepsilon_t (T_2 - T_1)] = \frac{EA(m_{c2}g)^2}{24} \left(\frac{\sum_{i=1}^n a_i^3}{\sum_{i=1}^n a_i} \right) \quad (3.43)$$

The expression

$$a_{id} = \sqrt{\frac{\sum_{i=1}^n a_i^3}{\sum_{i=1}^n a_i}} \quad (3.44)$$

is called the **equivalent span** or **ruling span** of a tensioning section. Using this term, it is obtained from (3.48) and (3.39) that

$$H_2^2 [H_2 - H_1 + \frac{EA(a_{id} m_{c1}g)^2}{24H_1^2} + EA \varepsilon_t (T_2 - T_1)] = \frac{EA(a_{id} m_{c2}g)^2}{24} \quad (3.45)$$

$$\sigma_2^2 [\sigma_2 - \sigma_1 + \frac{E(a_{id} m_{c1}g)^2}{24H_1^2 A^2} + E \varepsilon_t (T_2 - T_1)] = \frac{E(a_{id} m_{c2}g)^2}{24A^2} \quad (3.46)$$

Example 3: A tensioning section of a power line consists of six spans with the length 350, 200, 450, 275, 500 and 325 m. The conductor ACSR 300/50 is installed with a conductor tensile stress of 50 N/mm² at 10°C. The sag at 60°C in the span with 500 m length should be calculated.

The equivalent or ruling span following from (3.44) is

$$a_{id} = \sqrt{\frac{350^3 + 200^3 + 450^3 + 275^3 + 500^3 + 325^3}{350 + 200 + 450 + 275 + 500 + 325}} = 391.65 \text{ m}$$

For the conductor ACSR 300/50, $A = 353.7 \text{ mm}^2$; $m = 1.235 \text{ kg/m}$, $E = 77000 \text{ N/mm}^2$ and $\varepsilon_t = 18.9 \times 10^{-6} / \text{K}$ applies. The horizontal tensile force will be $353.7 \times 50 = 17685 \text{ N}$.

From (3.45),

$$H_2^2 [H_2 - 17685 + \frac{77000 (353.7)(1.235 \times 9.81 \times 391.65)^2}{24 \times 17685^2} + 77000(353.7)(18.9 \times 10^{-6})(60 - 10)] = \frac{77000 (353.7)(1.235 \times 9.81 \times 391.65)^2}{24 \times 17685^2}$$

Solving, $H_2 = 15575 \text{ N}$. The maximum sag in 500m long span is obtained with (3.18)

$$f_{Max} = \frac{15575}{1.235 \times 9.81} \left[\cosh \frac{1.235 \times 9.81 \times 500}{2 \times 12275} - 1 \right] = 24.39$$

For **Concentrated Loads**, the sag of a conductor with concentrated loads can be determined by making use of the equivalence between conductor sags and bending moments of an **equivalent beam** with equivalent loads. In this case, it applies for the sag $f = M/H$ where H is the conductor horizontal force and M is the moment.

It is obtained for a span with n concentrated loads G_i :

$$f_x = \frac{1}{H} \left[\frac{x(a-x)m_c g}{2} + x \sum_{i=1}^n \left(1 - \frac{s_i}{a} \right) G_i - \sum_{i=1}^n (x - s_i) G_i \right] \quad (3.47)$$

The maximum sag must not necessarily occur underneath a concentrated load. The horizontal tensile force H , unknown in equation (3.47), can be calculated with

$$L = \int_0^a \sqrt{1 + \left(\frac{dy}{dx} \right)^2} dx = \int_0^a \sqrt{1 + \left(\frac{V}{H} \right)^2} dx \quad (3.48)$$

The vertical component V can be considered as the transverse force Q_t according to the shear force diagram. As $(Q/H)^2 \ll 1$, the conductor length L is obtained from (3.48) that

$$L = \int_0^a \left(1 + \frac{1}{2} \frac{Q^2}{H^2} \right) dx = a + \frac{1}{2H^2} \int_0^a Q^2 dx \quad (3.49)$$

The equation (3.32) and (3.33) represent the relation between the conductor lengths in the conditions 1 and 2. If the conductor length according to (3.49) is used in these equations and products of terms with small order are neglected, it is obtained that

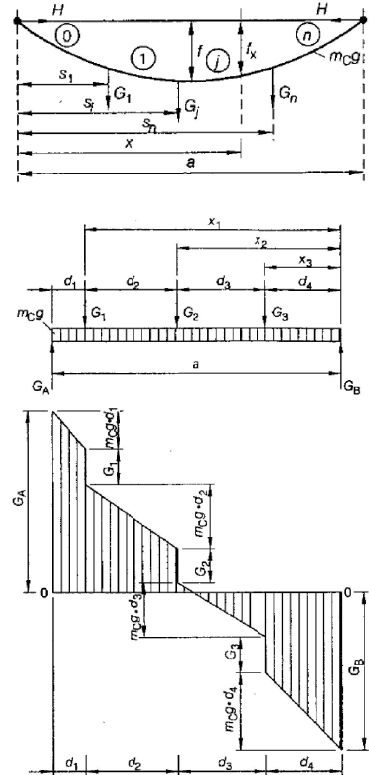
$$H_2^2 [H_2 - H_1 + \frac{EA}{2aH_1^2} \int_0^a Q_1^2 dx + EA \varepsilon_t (T_2 - T_1)] = \frac{EA}{2a} \int_0^a Q_2^2 dx \quad (3.50)$$

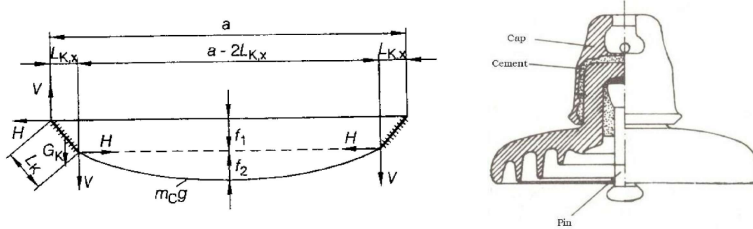
where Q_1 is related to condition 1, without concentrated loads, and Q_2 due to the condition 2, with concentrated loads. The integration can be carried out analytically, section by section, or by Simpson's rule, i.e.

$$\int_0^a Q^2(x) dx = \sum_{i=1}^n \frac{d_i}{3} (Q_{i-1}^2 + Q_i^2 + Q_{i-1} Q_i) \quad (3.51)$$

For a span with only one concentrated load G acting in the middle of the span, it is obtained

$$\int_0^a Q^2 dx = G^2 \frac{a}{4} + G m_c g a \frac{a}{4} + (m_c g a)^2 \frac{a}{12} \quad (3.52)$$





Consider also in a span with a short length and tension insulator sets at both ends, their effect on conductor tensile forces and sags cannot be neglected. In view of adequate consideration of the insulators, a distinction is to be made between rigid and flexible insulator sets. The first case corresponds to sets consisting of one long rod insulator, the second to an insulator set made of **cap-and-pin insulators** or with several **long rod insulator**. It applies to the case of a rigid insulator set

$$L_{K,x} = \frac{L_K}{\sqrt{1 + \left(\frac{V}{H}\right)^2}} \approx L_K \left(1 - \frac{1}{2} \left(\frac{V}{H}\right)^2\right) \quad (3.52)$$

The equivalent vertical load is in this case

$$V = \frac{1}{2} (m_{Cg}(a - 2L_{K,x}) + G_K) \approx \frac{1}{2} (m_{Cg}(a - 2L_K) + G_K) \quad (3.53)$$

Where G_K is the weight of the insulator set, L_K is the length of the insulator set, m_{Cg} is the weight of the conductor per unit length and $L_{K,x}$ is the length of the insulator set projected to the horizontal line.

For determination of conductor tensile force H_2 at a temperature T_2 and with the conductor mass per unit length m_{C2g} , the following formula for the conductor state change equation can be obtained.

$$\begin{aligned} H_2^2 [H_2 - H_1 + EA \varepsilon_t (T_2 - T_1) + \frac{EA}{H_1^2} \left[\frac{(m_{C1g})^2 (a - 2L_K)(a + 4L_K)}{24} + \frac{G_{K1} m_{C1g} L_K}{2} + \frac{G_{K1}^2 L_K}{4(a - 2L_K)} \right]] \\ = EA \left[\frac{(m_{C2g})^2 (a - 2L_K)(a + 4L_K)}{24} + \frac{G_{K2} m_{C2g} L_K}{2} + \frac{G_{K2}^2 L_K}{4(a - 2L_K)} \right] \end{aligned} \quad (3.54)$$

Comparing with (3.38), the term

$$H_2^2 [H_2 - H_1 + \frac{EA(a m_{C1g})^2}{24H_1^2} + EA \varepsilon_t (T_2 - T_1)] = \frac{EA(a m_{C2g})^2}{24} \quad (3.38)$$

$$\frac{(m_{Cg})^2 a^2}{24} \text{ is replaced by } \frac{(m_{C1g})^2 (a - 2L_K)(a + 4L_K)}{24} + \frac{G_{K1} m_{C1g} L_K}{2} + \frac{G_{K1}^2 L_K}{4(a - 2L_K)}$$

The sag consists of lowering of the insulator set and conductor sag in the middle of the span with f_1 and f_2 , where

Consider also in a span with a short length and tension insulator sets at both ends, their effect on conductor tensile forces and sags cannot be neglected. In view of adequate consideration of the insulators, a distinction is to be made between rigid and flexible insulator sets. The first case corresponds to sets consisting of one long rod insulator, the second to an insulator set made of cap-and-pin insulators or with several long rod insulator. It applies to the case of a rigid insulator set

$$f_1 = \frac{V}{H} L_{K,x} \quad f_2 = \frac{m_{Cg}}{8H} (a - 2L_{K,x})^2 \rightarrow f = \frac{V}{H} L_K \left[1 - \frac{1}{2} \left(\frac{V}{H} \right)^2 \right] + m_{Cg} \frac{(a - 2L_{K,x})^2}{8H} \quad (3.55)$$

A flexible insulator set can be simulated by a conductor section with a length according to the length of the insulator set L_K , where the weight force of the insulator set is assumed to be uniformly distributed. The conductor state change equation can be expressed as

$$H_2^2 \left\{ H_2 - H_1 + EA \varepsilon_t (T_2 - T_1) + \frac{EA}{H_1^2} \left[\frac{(m_{C1g})^2 a^2}{24} + G_{K1} m_{C1g} \frac{L_K}{2} + \frac{G_{K1}^2 L_K}{3a} \right] \right\} = EA \left[\frac{(m_{C2g})^2 a^2}{24} + G_{K2} m_{C2g} \frac{L_K}{2} + \frac{G_{K2}^2 L_K}{3a} \right] \quad (3.56)$$

where

$$\frac{(m_{Cg})^2 a^2}{24} \rightarrow \frac{(m_{C1g})^2 a^2}{24} + G_{K1} m_{C1g} \frac{L_K}{2} + \frac{G_{K1}^2 L_K}{3a}$$

Hence, the total sag is expressed as

$$f = \frac{1}{2H} \left(\frac{(m_{Cg})^2 a^2}{4} + m_{C1g} g L_K + G_K L_K \right) \quad (3.57)$$

Example 4: The sags at 40°C and -5°C with ice load of 10N/m should be calculated for a span of $a = 50m$ and a conductor ACSR 564/72. The insulator sets are assumed to be 5.0 m long and weigh 150 kg without ice load and 200 kg with ice load, respectively. The conductor tensile stress should be 10N/mm² at 10°C. The conductor cross section is 635.5 mm², the elastic modulus is 68kN/mm² and the coefficient of linear expansion is 19.4×10^{-6} . With (3.54), the equation is simplified to

$$\left(\frac{H_2}{1000} \right)^2 \left(\frac{H_2}{1000} - 6.3 + 25.1 + 207.9 \right) = 8396.5 \rightarrow H_2 = 6005N$$

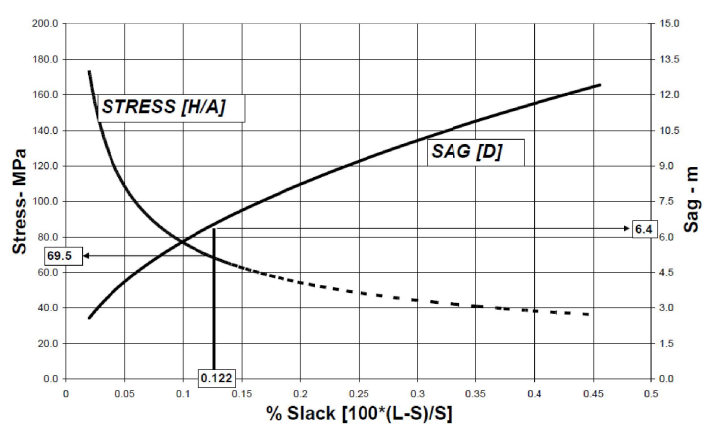
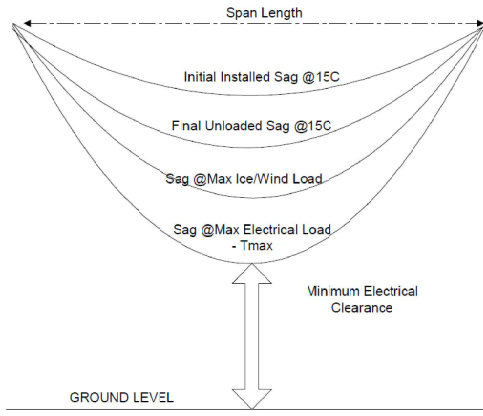
With $V = (2116 \times 9.81 \times 40 + 150 \times 9.81) / 2 = 1150.9N$, the sag in the middle can be represented by (3.55)

$$f = \frac{1150.9}{6005} (5.0) \left[1 - \frac{1}{2} \left(\frac{1150.9}{6005} \right)^2 \right] + (2.116)(9.81) \frac{(50 - 2(4.91))^2}{8(6005)} = 1.64 \text{ m}$$

and by (3.57), $f = 1.74 \text{ m}$.

While the conductor tensile forces are the same, the sag differs by 0.1m. For the condition -5°C with ice load, the conductor tensile forces can be calculated with (3.54) and (3.56) to be 9122 N and 9099 N respectively. The sags respectively are 1.54m and 1.64m.

As a summary, with cable weight, cable is sagged in form of a **hyperbolic cosine** or **parabolic**. Parabolic estimation assumes uniformly distributed load along span, instead of uniform weight along the cable itself. As the ground portfolio is never flat, i.e. in same level, **sag** and **tension** is calculated as functions along the span. Maximum sag is not located at the middle. Hence, the exact location with max sag is also found. With **elastic elongation** and **thermal elongation**, the conductor state change equation is derived. Power line is often tensioned with several span. Hence, an **equivalent span** or a ruling span representation is used to simplified the calculation. **Equivalent beam** with equivalent load method is employed for point load and the calculation is further developed to cater for **insulator weight**. It is noted that thermal annealing is often reason for elongation with wind load, ice load and power load.



Another approach is to represent length as a function of x ,

$$L(x) = \frac{H}{w} \sinh\left(\frac{wx}{H}\right) \approx x \left(1 + \frac{x^2 w^2}{6H^2}\right) \quad (3.58)$$

Slack is the difference between the total conductor length, L , and the chord distance between supports

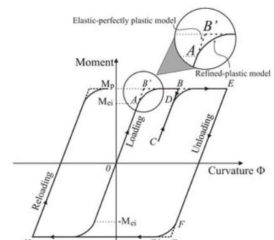
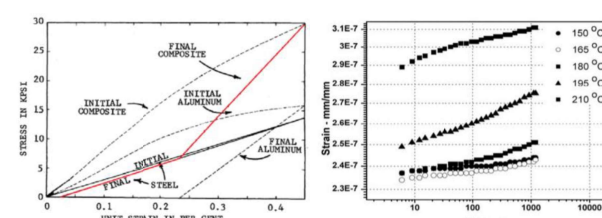
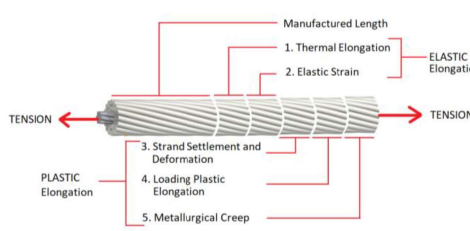
$$L - a = \left(\frac{2H}{w}\right) \sinh\left(\frac{wa}{2H}\right) - a \approx a^3 \left(\frac{w^2}{24H^2}\right) \approx f_{Max}^2 \left(\frac{8}{3a}\right) \quad (3.59)$$

Note: Accuracy of Sag Calculation depends on

1. **Uncertain weight of the conductor** – The **nominal weight** corresponds to the minimum acceptable weight. In reality, the weight of conductor typically exceeds the nominal value by 0.2% to 0.6%. Weight of wet conductor can exceed the dry weight by 2.5%
2. **End of Span Effect** – The equation assume that the conductor is fully flexible. If the **bending stiffness** of the conductor is taken into account, the actual sag in spans supported in suspension clamps is found to be less than that of catenary calculation.

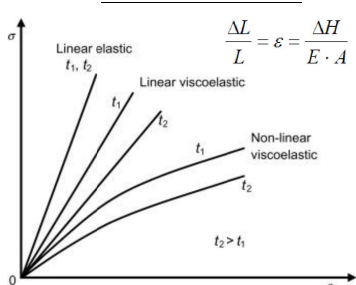
3. **Flexibility of Structures** – Changes in conductor tension at angle and dead-end strain structure causes elastic and inelastic structure deflections. If the resulting deflection of a dead-end structure in the preceding example is 1cm, the sag increases from 6.41 to 6.49 m, i.e. change of 1.2%. Pole structures may deflect more than steel lattice.
4. **Ice Load and Wind Load** - Limits on conductor tension can be expressed as a percentage of the conductor's rated tensile strength (RTS), as a conductor tension value, or as a catenary constant (H/w). Under high ice and wind loading, the conductor tension increases and, unless constrained by design, the conductors or supporting structures (plus splices and dead-end fittings) may fail.

Initial Unloaded Tension at 15°C [% RTS]	Max. Design Tension under ice & wind load [% RTS]	Max Design Tension under ice & wind load [kN]	Initial Sag at 15°C [m]	Final Sag at 100°C [m]
10	22.6	31.6	12.9	14.6
15	31.7	44.4	8.6	11.0
20	38.4	53.8	6.4	9.4
25	43.5	61.0	5.1	8.4

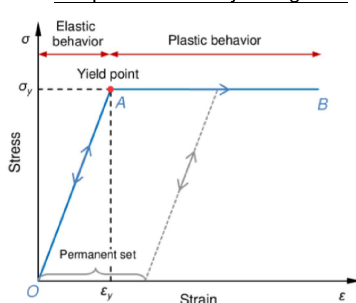


Modelling Conductor Elongation

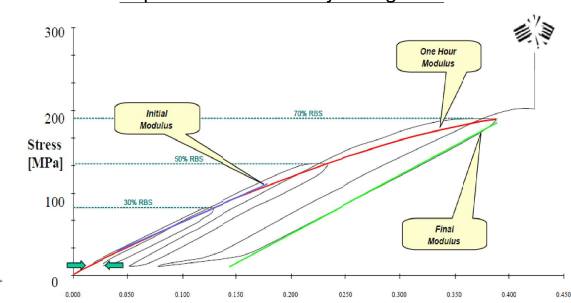
Linear Elastic Model

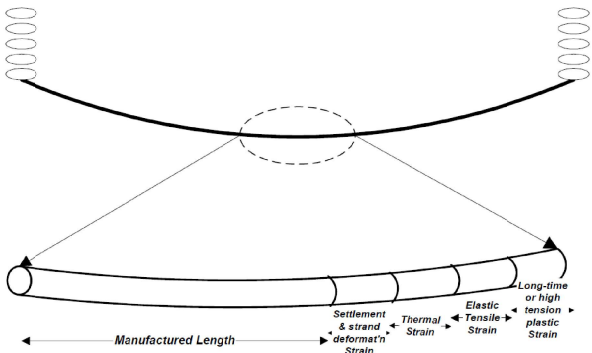


Simplified Plasticity Elongation



Experimental Plasticity Elongation





	Number of Strands	Elastic Modulus [GPa]
7	63.3	
19	61.2	
37	58.9	
61	58.3	

Al/Steel	Final Modulus [Gpa]	Steel Core Area [%]	Calculated Elastic Final Modulus [Gpa]
18/1	68.0	6%	62.5
22/7	71.0	9%	67.2
45/7	64.5	6%	63.7
54/19	69.7	11%	70.5

- The LE model ignores "settlement & strand deformation" as well as "long-time or high-tension plastic strain" (though such plastic elongation may be allowed for by the use of large clearance buffers).

Given the basic assumption on common elongation to different materials (A = Aluminum, S = Steel), i.e. $\varepsilon_{AS} = \varepsilon_A = \varepsilon_S$

$$\varepsilon_{AS} = \frac{H_{AS}}{A_{AS}E_{AS}} = \frac{H_A}{A_A E_A} = \frac{H_S}{A_S E_S} \rightarrow H_A = H_{AS} \frac{E_A A_A}{E_{AS} A_{AS}} \quad H_S = H_{AS} \frac{E_S A_S}{E_{AS} A_{AS}} \quad (3.60)$$

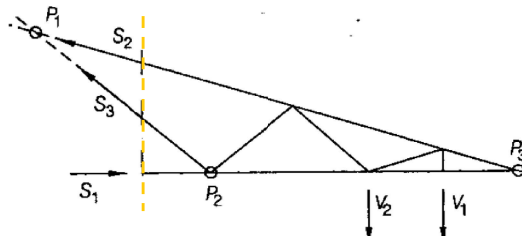
$$E_{AS} = E_A \frac{A_A}{A_{AS}} + E_S \frac{A_S}{A_{AS}} \quad (3.61)$$

The linear coefficient for thermal elongation is

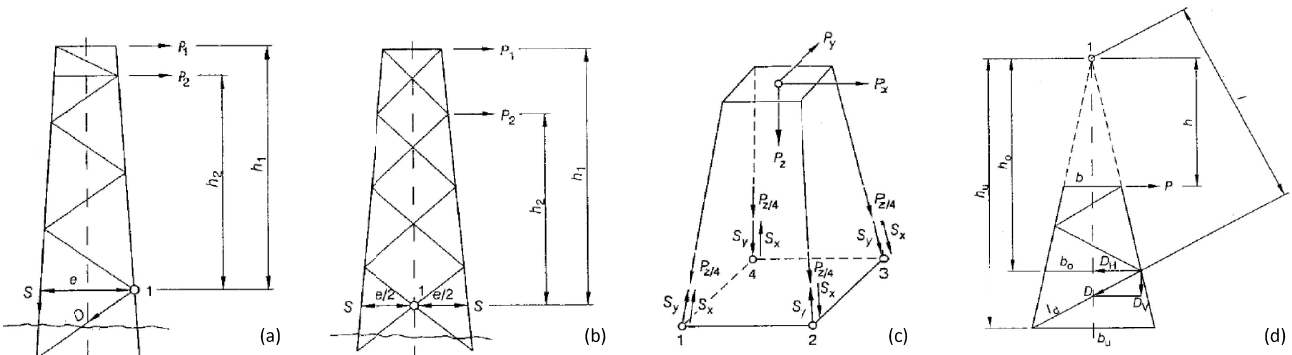
$$\alpha_{AS} = \alpha_A \frac{E_A}{E_{AS} A_{AS}} + \alpha_S \frac{E_S}{E_{AS} A_{AS}} \quad (3.62)$$

- The SPE model ignores the settlement and strand deformation that occur during initial tensioning of conductor but account for long-time or high tension creep plastic elongation by using a typical value of plastic conductor elongation (often expressed as a temperature "adder"). Plastic elongation of aluminum can be divided into 3 categories:
 - Strand Settlement & Deformation (Initial Plastic Elongation) – When first loaded to a tension of 15% to 25% RTS, during the process of stringing and sagging, the Al layer elongates plastically by an amount increases with tension.
 - Short Time High Tension Plastic Elongation (Design Loading Plastic Elongation) – After the conductor is sagged and clipped, ice and/or wind may raise the tension to higher level (30% - 80% RTS in short (1 hr to 24 hrs).
 - Long Time "Metallurgical" Creep Elongation (Creep Plastic Elongation) – Due to every moderate tension of 15% to 25% RTS.
- The EPE elongation model allows the engineer to calculate both settlement & strand deformation and long-time or high-tension plastic strain based on laboratory conductor test results and an assumed line design and load sequence. Plastic conductor elongation increases with initial installed tension and decreases the ratio of steel to aluminum cross sectional area.

3.2 Structural Analysis for Truss System



Lattice steel tower can be considered as 3D hyper-static truss systems. The individual member are mainly loaded by axial forces. Hence, assume there is no shear, bending and torsion, internal force can be calculated by cut-and-expose method. By utilizing symmetry in design, the 3D static system can be reduced to statically determined plane system.



Sectionalizing the truss, the leg member force S can be obtained from the equilibrium of moment around point 1: (Fig. a)

$$\sum P \cdot h = 2Se \sqrt{1 + \frac{\Delta^2}{4}} \rightarrow S = \frac{\sum P \cdot h}{2e \sqrt{1 + \frac{\Delta^2}{4}}} \quad (3.63)$$

For Fig. b, in case of symmetrical double warren, it can be assumed that both leg member forces are equal but in opposite direction. The equilibrium of moment around crossing point 1 results again in (3.63).

For Fig. d, the load P is distributed on two tower faces. The moment around point 1 yields

$$D = \frac{Ph}{2l} \quad (3.64)$$

The member force obtained by this procedure can act as a tensile or compressive force since the external load may act in both direction. In case of double warren, the member force are half of the value obtained from (3.63).

Since the determination of value h and l can be troublesome, the following transformation might be favorable.

$$Ph = 2 \left(D_H h_0 + \frac{D_V b_0}{2} \right) \quad (3.65)$$

or in general,

$$D = \frac{l_d}{2b_0 b_u} \sum Pb \quad (3.66)$$

The load created by asymmetrically acting vertical loads yields similar equations as (3.66).

$$D = \frac{\Delta l_d}{2b_0 b_u} \sum P_V b_V \quad (3.67)$$

where Δ designated the increase of latitude of the considered tower face per unit length. This equation applies only to bracing below the level of the acting force P_V .

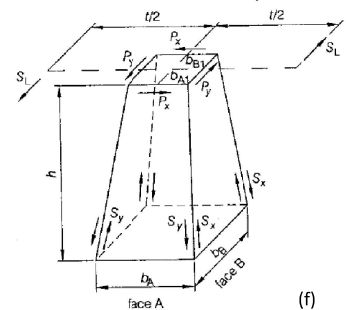
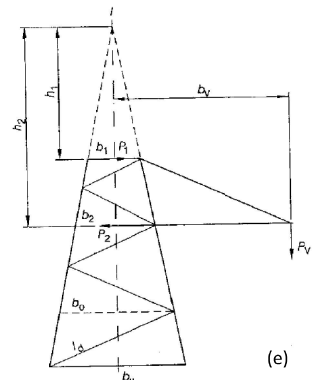
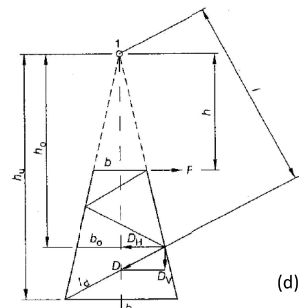
Loading of tower body by torsional moments is a **statically indeterminate** problem. Yet, simplifying assumptions for the distribution of torsional moment on the individual tower faces may be assumed if at all crossarm level and at changes of slope of leg member, horizontal bracing are provided and the ratio of the width of faces is not more than 1: 1.5 and the shape of tower is prismatic or corresponds to a truncated pyramid.

The load of the tower face by a torsional moment M_T should not result in leg member forces, i.e. the leg member forces S_x and S_y resulting from the force P_x and P_y should be equal and act in opposite direction (Fig. f), therefore,

$$P_x \frac{h}{b_A} = P_y \frac{h}{b_B}, \quad \frac{P_x}{P_y} = \frac{b_A}{b_B} = \frac{b_{A1}}{b_{B1}} \quad (3.68)$$

The torsional moment is obtained from

$$M_T = S_L t = P_x b_{B1} + P_y b_{A1} = P_y \left(\frac{b_{A1}}{b_{B1}} \right) b_{B1} + P_y b_{A1} = 2P_y b_{A1} \quad (3.69)$$



From these relations, it follows for P_x and P_y that

$$P_x = \frac{M_T}{2b_{B1}}, \quad P_y = \frac{M_T}{2b_{A1}} \quad (3.70)$$

Inserting P_x as external load in (3.66), the forces in the bracings of the tower face A are obtained as

$$\text{Torsion: } D_A = M_T \frac{b_{A1}}{b_{B1}} \frac{l_d}{2b_{A0}b_{Au}}, \quad D_B = M_T \frac{b_{B1}}{b_{A1}} \frac{l_d}{2b_{B0}b_{Bu}} \quad (3.71)$$

Combining also with the horizontal load, asymmetrical vertical load and torsions,

$$\text{Horizontal: } D = \frac{l_d}{2b_0 b_u} \sum Pb \quad (3.66)$$

$$\text{Vertical: } D = \frac{\Delta l_d}{2b_0 b_u} \sum P_V b_V \quad (3.67)$$

Total bracing force can be expressed as:

$$D_A = \left(\sum Pb + \Delta \sum P_V b_V + \sum M_T \frac{b_A}{b_B} \right) \frac{l_d}{2b_{A0}b_{Au}} \quad (3.72)$$

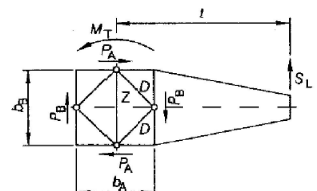
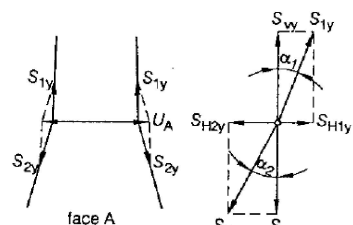
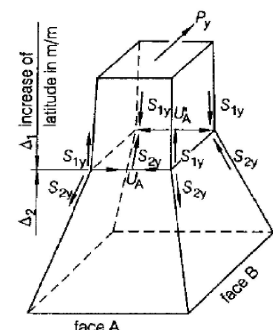
Lattice steel tower are frequently designed with a wide spread lower part with respect to the foundation forces. The horizontal forces produced by the change of leg member inclination have to be withstood by a horizontal bracing. When loaded by the force P_y , no force will occur in the horizontal member at the waist of face B. In face A, the horizontal force U_A will be

$$\begin{aligned} S_{H2y} &= S_{Vy} \tan \alpha_2 = S_{Vy} \frac{\Delta_{2A}}{2} \approx S_y \frac{\Delta_{2A}}{2} \\ S_{H1y} &= S_{Vy} \tan \alpha_1 = S_{Vy} \frac{\Delta_{1A}}{2} \approx S_y \frac{\Delta_{1A}}{2} \end{aligned} \quad (3.73)$$

$$U_A = S_{H2y} - S_{H1y} = S_y \frac{(\Delta_{2A} - \Delta_{1A})}{2} \quad U_B = S_x \frac{\Delta_{2B} - \Delta_{1B}}{2}$$

Horizontal bracings arranged at the level of lower crossarm chords in the tower body distribute the torsional moments resulting from the crossarms to the four faces of a tower body. The member D transfer a portion of the torsional moment to face B hence

$$P_B = S_L \frac{t}{2b_A} \rightarrow D = S_L \sqrt{b_A^2 + b_B^2} \frac{t - b_A}{4b_A b_B} \quad (3.74)$$

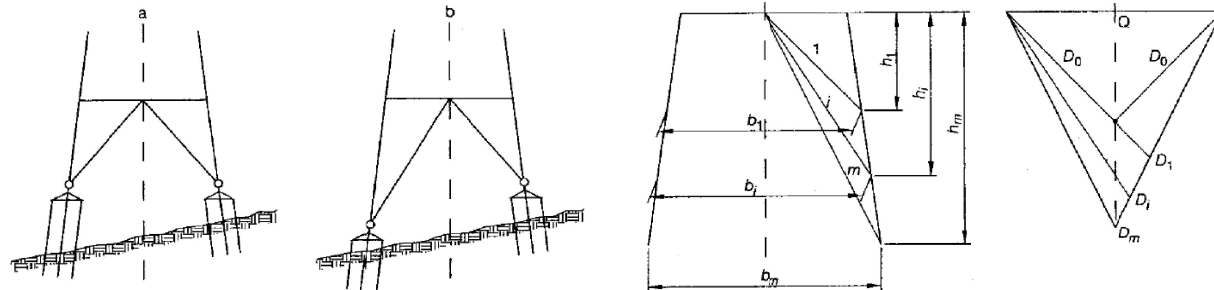


The foundation muff should be arranged as close as possible below the connection of lower bracing member to the corner leg to keep low the bending of the unsupported leg member resulting from the horizontal components of the bracing forces.

The extension of foundation muffs according to Fig. a requires a strong **concrete reinforcement**, especially in case of high differences in the ground surface. To avoid these expensive reinforcement, the connection of the lowermost bracing is arranged at the same height above ground for each individual tower leg, i.e. Fig b, with leg extension in different length. These differing leg extension needs to be considered when calculating the lower parts of the tower body, as the member forces and the **buckling length** of the member changes. Since the design is not symmetrical, the distribution of the loads on leg members and bracings changes as well. To limit the effort for calculation and design, leg extensions are provided with steps of 0.25 or 0.5 m and the design is based on the most unfavorable combination of leg extensions (Fig. c). As an approximation, the determination of forces can be carried out accordingly.

$$D_i = 2D_0 \frac{b_1}{b_i + h_i} \frac{\sqrt{b_i^2 + (2h_i)^2}}{\sqrt{b_i^2 + (2h_m)^2}} \quad (3.75)$$

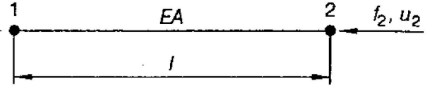
The member force D_0 is taken from the basic tower analysis. The maximum forces in the leg extensions result from the combination with the longest leg extension in each case.



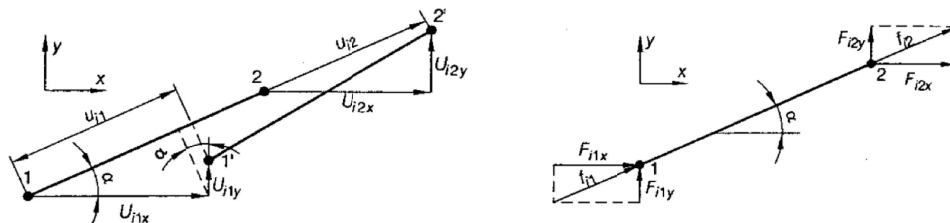
In fact, **Finite Element Method** represents an approach with systematic computation of any types of 3D, statically determined or hyperstatic truss structure. The complete structure is divided into element, the mechanical behavior of which is known.

Consider a truss element,

$$\begin{pmatrix} f_{i1} \\ f_{i2} \end{pmatrix} = \frac{EA}{L} \begin{pmatrix} 1 & -1 \\ -1 & 1 \end{pmatrix} \begin{pmatrix} u_{i1} \\ u_{i2} \end{pmatrix} \rightarrow \mathbf{f}_i = \mathbf{k}_i \mathbf{u}_i \quad (3.76)$$



It correlates force and displacement in each node with the member characteristics, inc. elasticity E, cross-sectional area A and length L.



The matrix \mathbf{k}_i is the stiffness matrix of element i in the local coordinate system.

The local element coordinates possess differing positions in global coordinates system. The position of an element in the overall structure is obtained by a transformation to the global coordinate system.

$$\begin{aligned} u_{i1} &= U_{i1x} \cos \alpha + U_{i1y} \sin \alpha \\ u_{i2} &= U_{i2x} \cos \alpha + U_{i2y} \sin \alpha \end{aligned} \quad (3.77)$$

The indices 1 and 2 are related to the two ends of the member i . (3.77) can be represented with

$$\mathbf{u}_i = \mathbf{T}_i \mathbf{U}_i \quad \mathbf{T}_i = \begin{pmatrix} \cos \alpha & \cos \alpha & 0 & 0 \\ 0 & 0 & \sin \alpha & \sin \alpha \end{pmatrix} \quad (3.78)$$

The matrix \mathbf{T}_i transfers displacements from the global coordinate system into the local one. With the fundamental assumption with only axial forces, force f_{i1} and f_{i2} can be related to the global coordinate x and y with

$$F_{i1x} = f_{i1} \cos \alpha; \quad F_{i1y} = f_{i1} \sin \alpha; \quad F_{i2x} = f_{i2} \cos \alpha; \quad F_{i2y} = f_{i2} \sin \alpha \rightarrow \mathbf{F}_i = \mathbf{T}_i^T \mathbf{f}_i \quad (3.79)$$

Putting (3.79) into (3.76),

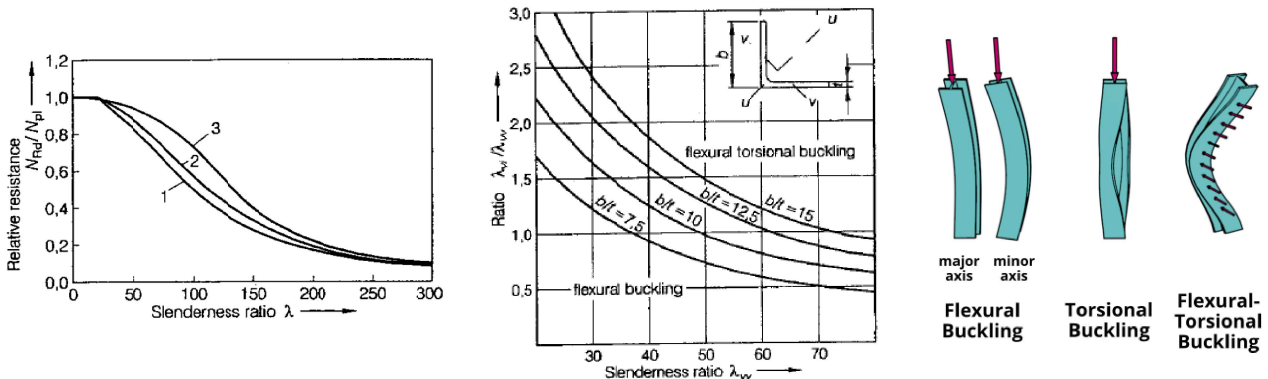
$$\mathbf{F}_i = \mathbf{T}_i^T \mathbf{k}_i \mathbf{u}_i = \mathbf{T}_i^T \mathbf{k}_i \mathbf{T}_i \mathbf{U}_i = \mathbf{K}_i \mathbf{U}_i \quad (3.80)$$

The relations between forces and displacements for the overall structure can be expressed by the format of (3.70); the number of node forces and displacements is increased then with U as the node displacement vector of overall structure in global coordinate system and K is the total stiffness matrix of the structure. It can be obtained by applying the direct stiffness method with

$$\mathbf{K} = \sum_i \mathbf{K}_i \quad (3.80)$$

With known force F_a and unknown force F_b , and unknown displacement U_a and known displacement U_b ,

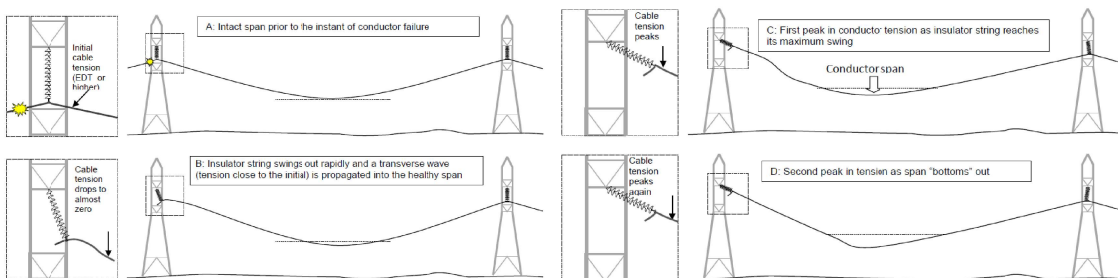
$$\begin{pmatrix} F_a \\ F_b \end{pmatrix} = \begin{pmatrix} K_{aa} & K_{ab} \\ K_{ba} & K_{bb} \end{pmatrix} \begin{pmatrix} U_a \\ U_b \end{pmatrix} \rightarrow F_a = K_{aa} U_a + K_{ab} U_b \rightarrow U_a = K_{aa}^{-1} (F_a - K_{ab} U_b) \quad (3.81)$$



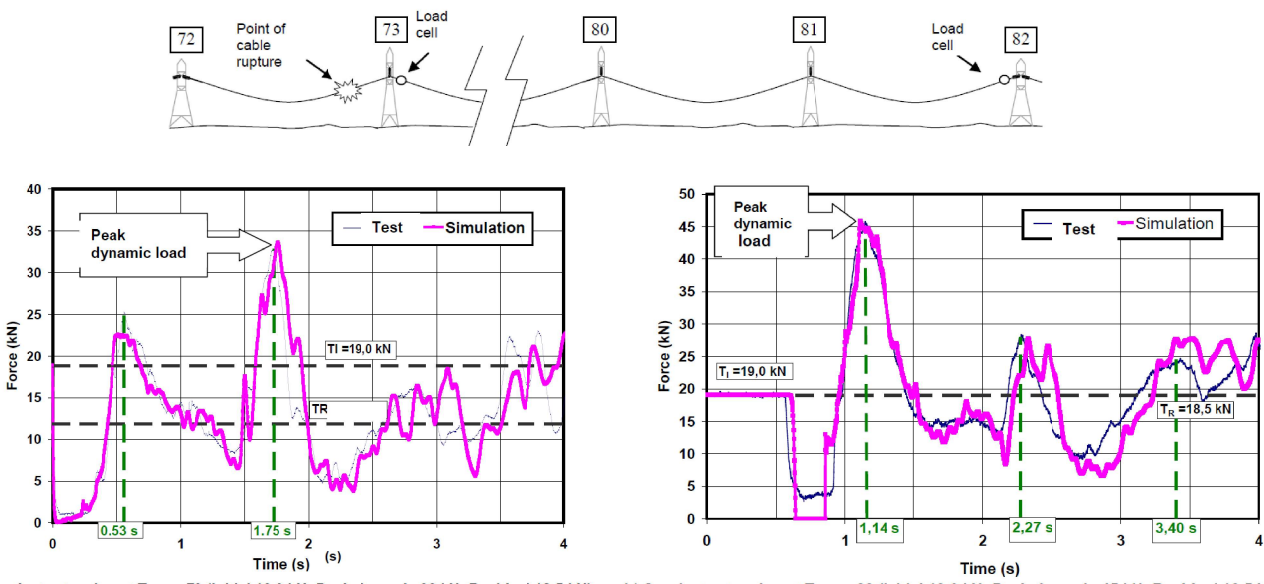
With long members with slenderness ratio $\lambda > 10$, it is prone to **buckling** instead of **compressive failure** when it is under axial load, or **torsional buckling** when it is under shear. It is noted that both **relative resistance** and **slenderness ratio** of flexural and flexural-torsional buckling decreases with increasing slenderness ratio. It also means the ease of buckling failure with long member and the requirement to reduce the length of member or with special design in cross-section geometry.

3.3 Structural Failure and Redundancy in Tower Structure

This initial transient dynamic response of the system in components immediately adjacent to the failure point, occurs within the first second or two following failure. Following this, return waves of ever decreasing magnitude are experienced as tension waves are reflected from support points, until the span comes to rest in a **residual static** (steady state). It may take several seconds (or even a few minutes depending on the initial impact) for the damaged line to finally stop oscillating.



The timing and relative magnitude of the first peaks in conductor tension will vary depending on **span geometry**, and not all research reports significantly higher peak loads during the second peak. The effect of the motion due to the transverse conductor wave at successive suspension supports is to decrease both the **peak dynamic load** (PDL) as well as the **residual static load** (RSL) experienced by successive towers.



Generally, the impact of the event on the tower and foundations is affected by:

- **The natural frequency of the tower and intact span(s)**

Craig (2006) on Structural Dynamics indicates that the global response of the tower to shock loads will depend on the **shape** of the impulse and more importantly on the **duration** of the impulse, t_d . If t_d is short compared to the natural period of the line system, T , (for $t_d/T \leq 0.15$) dynamic amplification factors remain small (often below 1.0) as the system is slow to react.

- **The response of lattice members to transient loads of short duration**

Natural period considered would be that of the individual tower member in the failure mode under consideration (axial, flexural or torsional). This is also a result of **strain rate effects**: steel usually exhibits higher strength and modulus of elasticity at high strain rates.

- The dispersion of the **failure shock** from the conductor support point into the superstructure

At conductor failure, shock load experienced at the conductor support point will flow through the superstructure into the main legs and foundation supports. Impact loads from lateral support points (exterior phases depending on tower top geometries or ground wire failures) may produce significant **torsional effects** in the tower. As with static loads, the magnitude of load experienced in the main legs is significantly affected by the base width of the structure.

Foundation response to the dynamic shock induced by the initial failure will depend on the internal force signature of the main legs as they are interfacing with the foundation. The foundation (its structure and the surrounding soil/rock) will react to the shock according to their own dynamic characteristics (typically lower dominant natural frequency and higher damping than the superstructure). Typically, rock foundations with higher **stiffness** will be more prone to shock loads than softer foundation types.

- Soil-structure interactions**

Impact of dynamic loads on the support may be decreased when soil-structure interactions are considered. From a static perspective, the presence of elastic foundation material will slightly reduce the impact load: Conventional footings in **cohesive soils**, will provide more flexibility (accommodate **larger displacements**) than **granular soils**, while supports in rocky soils will act as rigid supports.

To accurately predict the **peak dynamic loads** (PDL) and **residual static load** (RSL) due to conductor breakage, the following parameters should be considered.

- Conductor Tension

Strain energy stored in the conductor in the intact profile is the primary source of KE following the broken wire event. Larger energy releases induce larger accelerations, and greater inertia forces and motions, and larger PDL.

Conductor with larger **weight**, or under **sustained overload** will also result in a higher RSL.

Suspension I- or V-string insulators swing out, thus increasing the available slack and decreasing the RSL. However suspended spans will experience a **second peak dynamic load** as the healthy span "bottoms out" following conductor failure, which will increase the PDL (as it will be governed by the second peak).

The assembly type also affects the **load application rate**. Towers fitted with **suspension assemblies** will initially see no load until the suspension assembly swings out, however **strain assemblies** will transfer an instantaneous step change or **shock load** propagated by the failure.

Longer suspension strings, and specifically the **ratio of suspension string length to slack**, decrease the RSL. The same ratio may have the effect of increasing the PDL as the injection of more slack into the healthy section will allow further acceleration before the healthy section "bottoms out".

Number of suspension spans to the next strain point will tend to increase the RSL, since successive suspension sets also swing out, thus reducing the net slack length injection into the healthy span. However, the energy dissipated by successive suspension sets also moving will decrease the PDL. These effects typically saturate after about four spans.

Spans with lower span to sag ratios tend to produce a higher PDL and RSL.

PDL decreases with a decrease in span length (and more for flexible supports). A shorter span adjacent to the breakage point promotes dynamic interactions with successive spans, especially the second one.

- Length of Suspension Insulator String

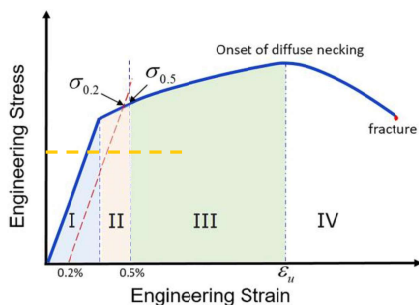
- Number of Suspension Spans from the Assessed Tower to the Next Dead-End Structure

- Span / Sag Ratio

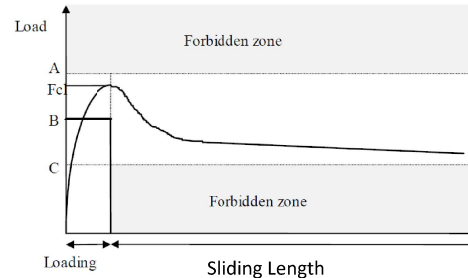
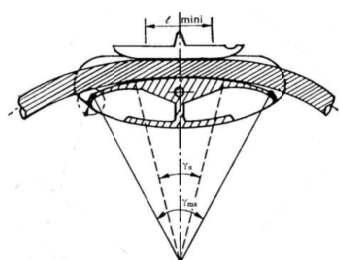
- Span length

Mitigation Measures for OHL Cascade Failure

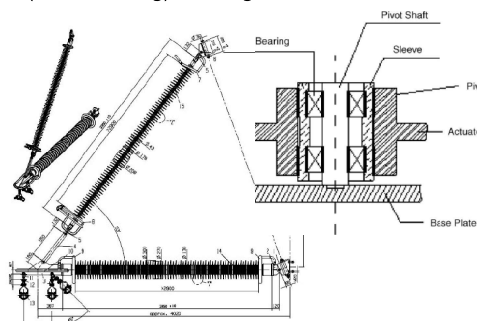
- Post-Elastic Reserves



- Sliding Clamps



- (Load Limiting) Pivoting Cross-Arm



- Anti-Cascading Tower

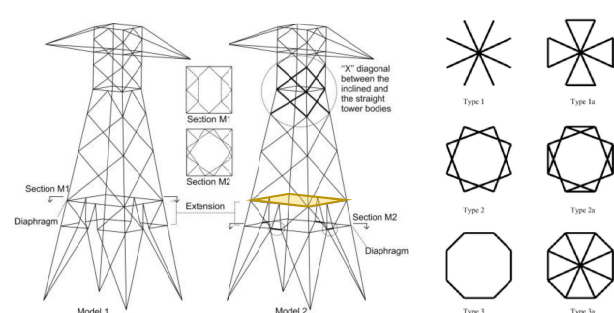


- Overhead Line De-icing



Diaphragm, which is to reduce the chance of vibration failure and buckling failure, is also employed to with member redundancy.

The goal is to add a series of diaphragm bracing types at mid-height of the slender diagonal members. The problem is to identify the type, the internal nodes and location of diaphragms.

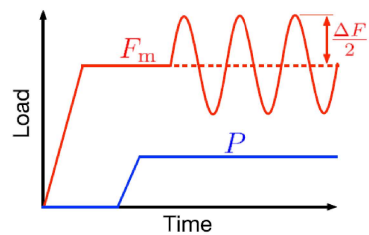


3.4 Fretting Failure

Overhead conductors are frequently subjected to **aeolian vibration**, which is a major cause of fatigue failure in conductors. The failure usually takes place near components where the movement of the conductor is restrained, such as suspension clamps, spacer dampers, vibration dampers, and strain clamps. In these fatigue critical regions, the wires of the conductor are subjected to complicated stress histories caused by the combination of aeolian vibration and static stresses due to the **clamping pressure**, **stretching load**, and **weight** of the span. The wires are subjected to surface damage induced by relative **tangential displacements**.

Wire failure is usually caused by fretting fatigue damage, that different fretting regimes (**stick**, **partial slip**, **gross sliding**) occur in wires of a conductor, and that there is a critical region in the conductor clamp assembly where wire breaks are most frequent. The factors that affect the fatigue performance of conductors are **wire material**, **clamp geometry**, **mean load**, and **vibration amplitude**.

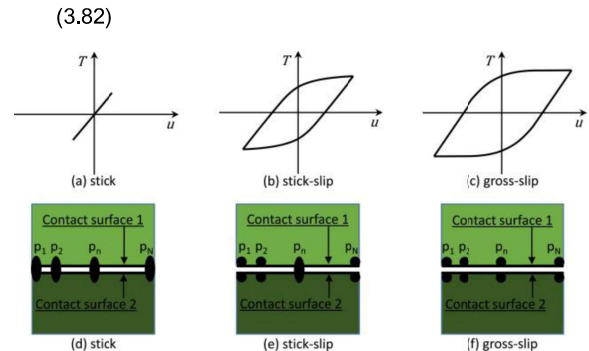
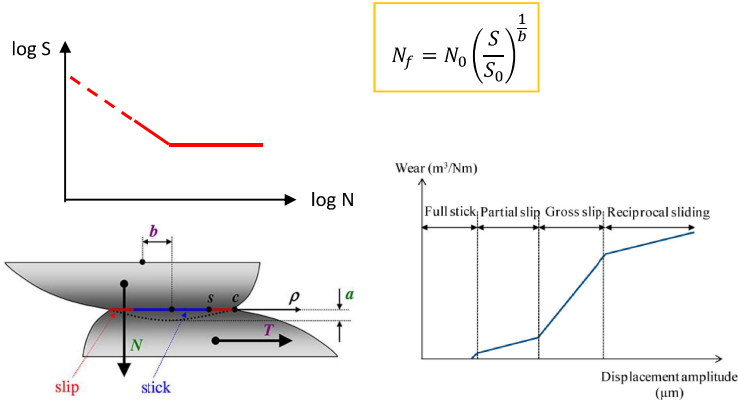
Fatigue life of wires can be affected by the **normal force** and **crossing angle** and that a corrosive atmosphere can affect wear damage and fretting regime. Numerical models have also allowed the estimation of **contact pressure**, **contact area**, **crack initiation site**, and **fatigue life** of wires.



Fatigue Model:

1. Basquin's Law:

Number of Cycle to Fracture $N_f = f(S, S_0, N_0, b)$, where S = Applied stress range = $\Delta\sigma = 2\sigma_a$ (N_0 , S_0) = Point on the material curve, b = Fatigue strength exponent.



2. Mean Stress Correction

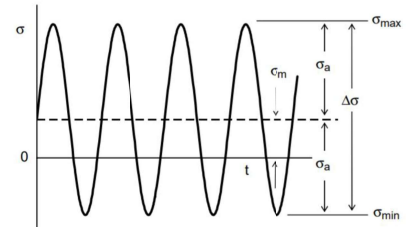
For fatigue loadings that have small mean stress compared to the alternating stress, the theories show little difference.

Goodman presents the corrected stress amplitude σ'_a

$$\left(\frac{\sigma_a}{\sigma'_a}\right) + \left(\frac{\sigma_m}{\sigma_u}\right) = 1 \rightarrow \sigma'_a = \frac{\sigma_a}{1 - \frac{\sigma_m}{\sigma_u}} \quad (3.83)$$

Gerber and Soderberg suggests:

$$\text{Gerber: } \left(\frac{\sigma_a}{\sigma'_a}\right) + \left(\frac{\sigma_m}{\sigma_u}\right)^2 = 1, \quad \text{Soderberg: } \left(\frac{\sigma_a}{\sigma'_a}\right) + \left(\frac{\sigma_m}{\sigma_y}\right) = 1 \quad (3.84)$$



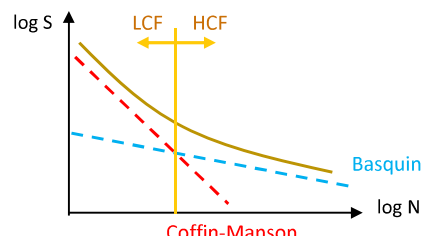
3. Basquin-Coffin-Manson Law:

$N_f = f(\sigma_f, b, \varepsilon_f, c)$ σ_f = Fatigue strength coefficient, b = Fatigue strength exponent, ε_f = Fatigue ductility coefficient, c = Fatigue ductility exponent

$$\frac{\Delta\varepsilon}{2} = \frac{\sigma_f}{E} (2N_f)^b + \varepsilon_f (2N_f)^c \quad (3.85)$$

4. Smith-Toppert-Watson Law: accounts for mean stresses by using a damage parameter gathered from the maximum stress at each cycle.

$$\sigma_{max}\varepsilon_a = \frac{(\sigma_f')^2}{E} (2N_f)^{2b} + \sigma_f' \varepsilon_f (2N_f)^{b+c} \quad (3.86)$$

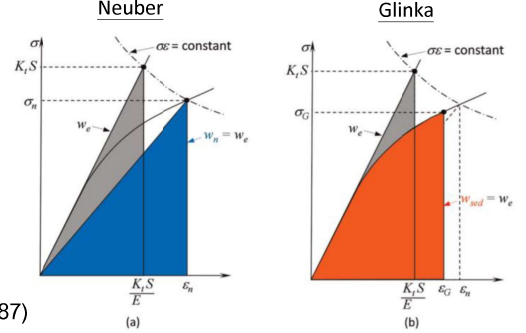


The **linear elastic calculations** done to acquire the stresses and strains are usually done according to **Hooke's law** of a linear stress-strain relationship. This may erroneously give higher stresses than yield stresses *locally*, not only at the **crack tips**, but also in small regions in the model.

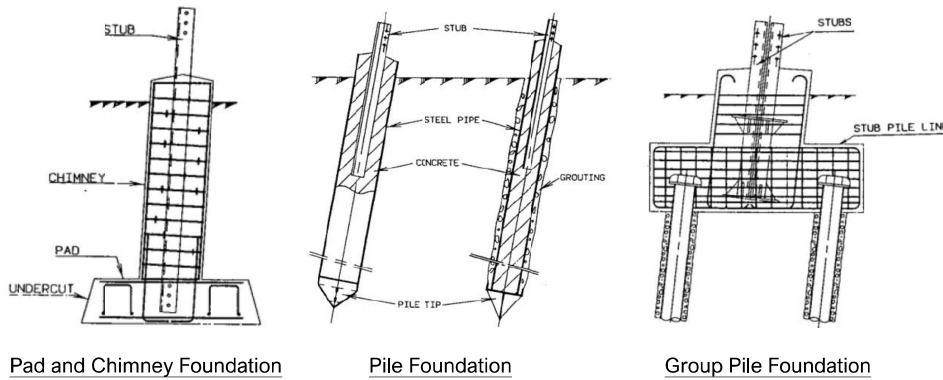
Correction for plasticity can be done by different versions of the Neuber formulae:

- Local or nominal
- Neuber (implemented in ANSYS fatigue module)
- Elastic Strain Energy Density (ESED)

$$\text{Neuber: } E\varepsilon = \sigma / \sqrt{1 - \left(\frac{\sigma}{\sigma^*}\right)^2} \quad (3.87)$$



3.5 Foundation for Transmission Tower



When analyzing the ultimate limit state, the undrained condition the **uplift capacity** of a spread foundation governs, and is given by Kulhawy (1995) as

$$Q_u = Q_{su} + Q_{tu} + W \quad (3.88)$$

where Q_u is the uplift capacity, Q_{su} is the side resistance, Q_{tu} is the tip resistance, and W is the weight of foundation and enclosed soil as shown schematically.

Q_{su} can be calculated as

$$Q_{su} = 2(B + L) \int_0^{D_1} \bar{\sigma}_v(z) K(z) \tan \bar{\phi}(z) dz \quad (3.89)$$

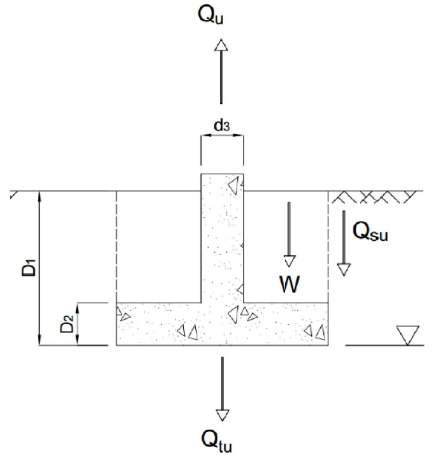
where B is the foundation width, L is the foundation length, D_1 is the foundation depth, $\bar{\sigma}_v(z)$ is the vertical effective stress, $K(z)$ is the operative horizontal stress coefficient, $\bar{\phi}(z)$ is the effective stress friction angle, and z is the depth.

The tip resistance, Q_{tu} , can be calculated as

$$Q_{tu} = (-\Delta u - u_i) A_{tip} \quad (3.90)$$

where Δu is the change in pore water stress by undrained loading, u_i is the initial pore water stress at the foundation tip or base and A_{tip} is the tip or base area. A single equation for the performance function P of the foundation can then be formed in the ultimate limit state as

$$P = Q_u - F \quad (3.91)$$



where F is the foundation reaction determined from the external loads. The three possible outcomes of this equation, $P = 0$, $P < 0$ and $P > 0$, allow a quantifiable analysis of the foundation performance.

Kulhawy (1995) developed the following simple hyperbolic model for the relation between Uplift load F , Uplift Capacity Q_u , and vertical displacement y .

$$\frac{F}{Q_u} = \frac{y}{a + by} \quad (3.92)$$

where a and b are curve-fitted parameters. (3.92) is based on the idea of normalising load-displacement curves to obtain a single representative curve for design purposes. This was done using trial and error analysis of available load-displacement data. Displacement at 50% of the failure load, y_{50} , and the displacement at failure, y_f , give the constant a and b with

$$a = \frac{y_{50} y_f}{y_f - y_{50}} \quad b = \frac{y_f - 2y_{50}}{y_f - y_{50}} \quad (3.93)$$

The serviceability limit state is defined as that in which the undrained uplift displacement is equal to the allowable limit imposed by the structure. A performance function analogous to (3.91) for the ultimate limit state is given by

$$P = Q_{ua} - F, \quad Q_{ua} = \frac{Q_u y_a}{a + by_a} \quad (3.94)$$

where Q_{ua} is the allowable uplift capacity based on a given displacement limit, y_a .

The three possible outcomes of equation (3.94), again analogous to equation (3.91), represent the definition of the serviceability limit state if $P = 0$, an unsatisfactory foundation if $P < 0$ and a satisfactory foundation if $P > 0$.

Given that exact ground conditions are often not well defined, a nominal strength that uses conservative estimates of the material properties can be adopted. An equation analogous to equation (3.94) for the nominal allowable uplift capacity, Q_{uan} is then

$$Q_{uan} = \frac{Q_{un} y_a}{m_a + m_b y_a} \quad (3.95)$$

where m_a ($=7.13$) and m_b ($=0.75$) are the mean values of a and b respectively and Q_{un} is given by

$$Q_{un} = Q_{sun} + Q_{tun} + W, \quad Q_{sun} = 2(B + L) D_1 m_K \bar{\sigma}_{vm} \tan \bar{\phi}, \quad Q_{tun} = W - u_i A_{tip} \quad (3.96)$$

where B is the foundation width, L is the foundation length, D_1 is the foundation depth, $\bar{\sigma}_{vm}$ is the average vertical effective stress, and $\bar{\phi}$ is the effective stress friction angle.

The basic design formula for any component of the structure or line considered is given as

$$E_d \leq R_d \quad (3.97)$$

where E_d = design force and R_d = design resistance.

3.6 Equation of Motion – Dynamic Modelling

Consider the dynamic response $u(t)$ of a linear system with single degree of freedom. It is governed by a second order differential equation,

$$m\ddot{u} + c\dot{u} + ku = F(t) \quad (3.98)$$

The physical system parameters are mass m , viscous damping coefficient c and stiffness k .

Given the natural angular frequency ω_0 and damping ratio ζ , (3.98) can be further written as

$$\ddot{u} + 2\zeta\omega_0\dot{u} + \omega_0^2u = f(t) \quad (3.99)$$

with

$$\omega_0 = \sqrt{\frac{k}{m}} \quad \zeta = \frac{c}{2\sqrt{km}} \quad (3.100)$$

With fluctuating loads such as winds applied to a structure, there is a possibility that if the load frequency is close to the **natural frequency** of the structure, **resonance** causing large displacements may occur. When the external force is sinusoidal in nature over a single frequency then the resulting excitation is said to be **harmonic**.

For a SDOF system exposed to forced vibration, the equation of motion is given by Clough (1975),

$$\ddot{u} + 2\zeta\omega_0\dot{u} + \omega_0^2u = f_0 \sin(\omega t) \quad (3.101)$$

To solve this equation, the displacement u is expressed in form of

$$u = Re\{X_0 e^{j\omega t}\} \quad (3.102)$$

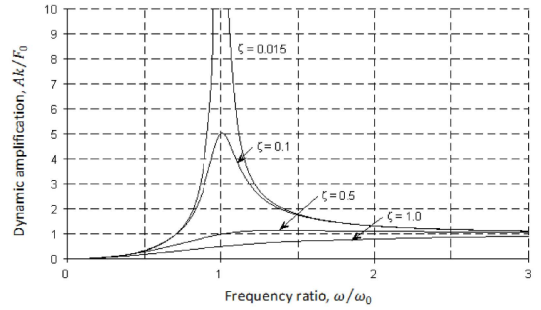
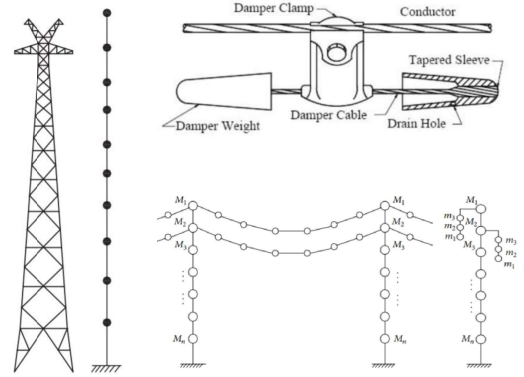
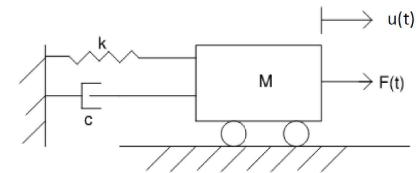
Hence, $(-\omega^2 + 2j\zeta\omega_0\omega + \omega_0^2)X_0 e^{j\omega t} = f_0 e^{j\omega t}$ (3.103)

The frequency response of X_0 can be represented by

$$X_0 = H(\omega)f_0 = \frac{f_0}{\omega_0^2 - \omega^2 + j2\zeta\omega_0\omega} \quad (3.104)$$

with

$$|H(\omega)| = \frac{1}{\sqrt{(\omega_0^2 - \omega^2)^2 + (2\zeta\omega_0\omega)^2}}, \quad \angle H(\omega) = \tan^{-1}\left(\frac{2\zeta\omega_0\omega}{\omega_0^2 - \omega^2}\right) \quad (3.105)$$



Consider the response of a SDOF system given by equation (3.98) exposed to a pulse with magnitude F_0 starting at $t = 0$ and ending at $t = t_1$, when $t \leq t_1$, there is a transient solution to the homogenous equation:

$$u_1(t) = e^{-\zeta\omega_0 t}(C_1 \sin(\omega_0 t) + C_2 \cos(\omega_0 t)) \quad (3.106)$$

The steady state solution of the equation is given by

$$u_2(t) = \frac{F_0}{k} \quad (3.107)$$

Using superposition for linear equation,

$$u(t) = u_1(t) + u_2(t) = e^{-\zeta\omega_0 t}(C_1 \sin(\omega_0 t) + C_2 \cos(\omega_0 t)) + \frac{F_0}{k} \quad (3.108)$$

Consider the initial displacement u_0 and \dot{u}_0 , for $t = 0$,

$$u_0 = \frac{F_0}{k} + C_2, \quad \dot{u}_0 = \omega_d C_1 + \omega_0 C_2 \quad (3.109)$$

The solution of equations (3.109) can now be written as

$$u(t) = e^{-\zeta\omega_0 t} \left(\frac{\dot{u}_0 + \zeta\omega_0(u_0 - \frac{F_0}{k})}{\omega_d} \sin(\omega_0 t) + \left(u_0 - \frac{F_0}{k} \right) \cos(\omega_0 t) \right) + \frac{F_0}{k} \quad 0 \leq t \leq t_1 \quad (3.110)$$

With an impulse force with magnitude F_0 and duration t_1 which goes towards zero and using the impulse-momentum theorem,

$$F_0 t_1 = m\ddot{u}_0(t_1) \quad (3.111)$$

The pulse will give the mass an initial velocity but no initial displacement to give

$$\dot{u}_0 = \frac{F_0 t_1}{m} \quad (3.112)$$

The infinitely short duration of steady-state response is succeeded by the free vibration described in (3.106). The solution to this known initial velocity with initial position = 0 can be given as

$$u(t) = e^{-\zeta\omega_0 t} \frac{\dot{u}_0 + \zeta\omega_0 u_0}{\omega_d} \sin(\omega_d t) = e^{-\zeta\omega_0 t} \frac{F_0 t_1}{m\omega_d} \sin(\omega_d t) \quad (3.113)$$

where ω_d is the damped natural angular frequency given by $\omega_d = \omega_0 \sqrt{1 - \zeta^2}$ (3.114)

Consider one of the infinitesimally small pulse loads of duration dt at time $t = \tau$. At $t = t_c$, the contribution of this load to the response of the system is given by

$$du(t_c) = e^{-\zeta\omega_0(t_c - \tau)} \left(\frac{f(\tau)dt}{m\omega_d} \sin \omega_d(t_c - \tau) \right) \quad (3.115)$$

The total contribution of the load to the system can be given by the summation of sequence of infinitesimally small pulse loads to compute a total solution at time $t = t_c$.

$$u(t_c) = \frac{1}{m\omega_d} \sum_{i=1}^n e^{-\zeta\omega_0(t_c-\tau)} f(\tau_i) d\tau \sin \omega_d(t_c - \tau_i) \quad (3.116)$$

where n is the number of pulse before the time t_c . As $d\tau \rightarrow 0$, the summation is transformed into an integral.

$$u(t_c) = \frac{1}{m\omega_d} \int_0^{t_c} e^{-\zeta\omega_0(t_c-\tau)} f(\tau) \sin \omega_d(t_c - \tau) d\tau \quad (3.117)$$

This is the Duhamel Integral and is usually written in form of

$$u(t_c) = \frac{1}{m\omega_d} \int_0^t e^{-\zeta\omega_0(t-\tau)} f(\tau) \sin \omega_d(t - \tau) d\tau \quad (3.118)$$

In contrast to a SDOF system, a multi degree of freedom (MDOF) system allows any number of moving parts to move or rotate in up to six directions at any given point.

The dynamic equation of motion for a MDOF system excited by a dynamic force can be written in matrix form as

$$[M]\ddot{\mathbf{u}} + [C]\dot{\mathbf{u}} + [K]\mathbf{u} = \mathbf{f}(t) \quad (3.119)$$

where $[M]$ is the mass matrix, $[C]$ is the damping matrix, $[K]$ is the stiffness matrix and \mathbf{u} is the displacement vector.

3.7 Aeolian Oscillation and Galloping

Wind forces acting transversely on the conductor cause alternating excitations in the vertical direction resulting in **Aeolian Vibrations**. They are characterized by relatively short wavelengths and frequencies between 5 and 100Hz with **laminar wind** with velocity 5 – 10m/s. It belongs to the **vortex-induced vibrations** and is classified as high frequency.

For long period of time, Aeolian Vibrations have been the subject of intensive studies. The mechanic model is related to a span with length a . Thereby, the coupling between adjacent spans by the insulator sets is neglected and the conductor sag is low compared with span length. Then, the conductor is strung between two attachment points mathematically replaced by a string with small **bending stiffness**. This model can be described by the PDE.

The model

$$EI \frac{\partial^4 \omega}{\partial x^4} - H \frac{\partial^2 \omega}{\partial x^2} + m_c \frac{\partial^2 \omega}{\partial t^2} = q_w(x, t) + q_d(\omega, \dot{\omega}, t) \quad (3.120)$$

The term $q_w(x, t)$ represents the force due to wind flow and the term $q_d(\omega, \dot{\omega}, t)$ the damping force due to conductor self-damping. For further considerations, it suffices to consider the free oscillations only. Therefore, the right side in (3.120) can be set to zero.

The remaining differential equation can be separated by the expression

$$\omega(x, t) = \omega(x) \sin \omega t \quad (3.121)$$

where $\sin \omega t$ is a solution of the time equation

$$\ddot{q}(t) + \omega^2 q(t) = 0 \quad (3.122)$$

Inserting (3.121) into (3.122) the spatial equation is obtained.

$$EI(\omega'')''(x) - H\omega''(X) - \omega^2 \omega(x) = 0 \quad (3.123)$$

There, $\omega(x)$ is the angular frequency of considered vibration mode.

For further considerations, the time-related component of the complete solution is without significance; therefore, only the spatial equation (3.123) needs to be studied. By using the set of solutions

$$\omega(x) = K e^{rx} \quad (3.124)$$

inserted into (3.123), the characteristics equation

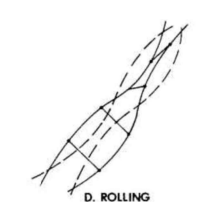
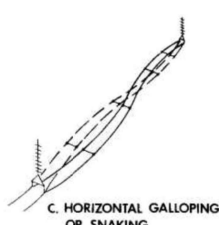
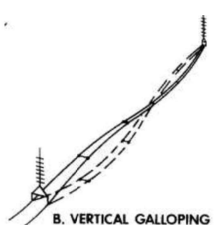
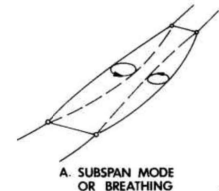
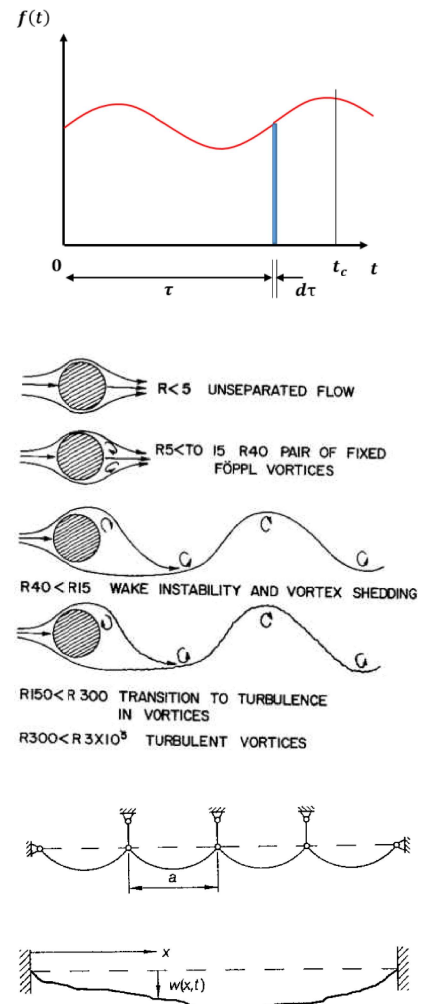
$$r^4 - \left(\frac{H}{EI}\right)r^2 - m_c \frac{\omega^2}{EI} = 0 \quad (3.125)$$

is obtained, the solutions of which are

$$r_{1,2,3,4} = \pm \sqrt{\frac{H}{2EI}} \pm \sqrt{\frac{m_c \omega^2}{EI} + \left(\frac{H}{2EI}\right)^2} = \pm \sqrt{\frac{H}{2EI}} \sqrt{1 \pm \sqrt{1 + \frac{4EIm_c \omega^2}{H^2}}} \quad (3.126)$$

Since the inner root > 1 , two real root $r_{1,2} = \pm \alpha$, $r_{3,4} = \pm j\beta$ with natural values

$$\alpha = \sqrt{\frac{H}{2EI}} \sqrt{\sqrt{1 + \mu} + 1} \quad \beta = \sqrt{\frac{H}{2EI}} \sqrt{\sqrt{1 + \mu} - 1} \quad \text{with } \mu = \frac{4EIm_c \omega^2}{H^2} \quad (3.127)$$



has been used. The corresponding integration constant can be obtained from the boundary conditions, finally finding the location-dependent displacement $w(x)$.

$$w(x) = C_1 \cosh \alpha x + C_2 \sinh \alpha x + C_3 \cos \beta x + C_4 \sin \beta x \quad (3.128)$$

A numerical study, taking into account the conductor usually used for overhead line together with the corresponding tensile forces and vibration frequencies, demonstrated that μ is small compared with 1. Therefore, the approximations

$$\alpha = \sqrt{\frac{H}{EI}} \quad \beta = \omega \sqrt{\frac{m_c}{H}} \quad (3.129)$$

can be accepted. Taking into account $\mu \leq 1$ and $\alpha \geq \beta$, it is obtained from (3.128) and (3.121).

$$\omega(x) = \hat{A}_f \sin \beta x \quad (3.130)$$

as an approximation for the location dependent displacement, where \hat{A}_f is the free-span amplitude. Assuming, that the conductor stiffness is negligible, the approximated solution of the frequency equation is, independently of the boundary conditions,

$$\sin \beta a = 0 \rightarrow \beta = \frac{k\pi}{a} \quad (3.131)$$

with k being natural numbers $k = 1, 2, 3 \dots$ (3.131) and (3.127) deliver the natural frequency, taking into account the bending stiffness,

$$f_s = \frac{k}{2a} \sqrt{\frac{H}{m_c}} \sqrt{1 + \frac{(k\pi a)^2 EI}{H}} \quad (3.132)$$

or, when the stiffness EI is neglected,

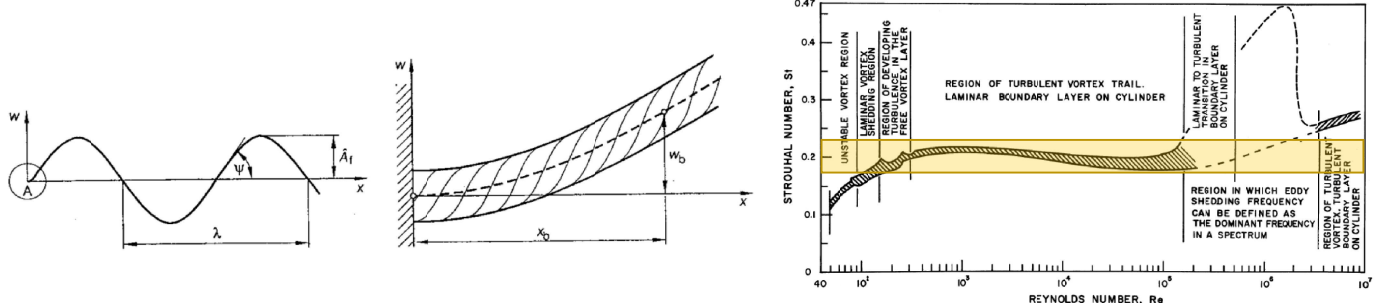
$$f = \frac{k}{2a} \sqrt{\frac{H}{m_c}} \quad (3.133)$$

(3.133) corresponds to the well-known expression for the natural frequencies of a string rigidly fixed at the both ends and, in practice, is adopted for overhead line conductors as well. The expression under the root in (3.133) represent the travelling wave velocity c when neglecting the bending stiffness, (or including bending stiffness)

$$c = \sqrt{\frac{H}{m_c}}, \quad c_s = \sqrt{\frac{H}{m_c}} \sqrt{1 + \frac{(k\pi a)^2 EI}{H}} \quad (3.134)$$

The relation between the order number k , also called harmonic coefficient, the span length a and the wavelength λ is

$$\frac{k}{2a} = \frac{1}{\lambda} \rightarrow \lambda = \frac{1}{f} \sqrt{\frac{H}{m_c}}, \quad \lambda_s = \sqrt{\frac{H}{2m_c f_s^2} + \sqrt{\left(\frac{H}{2m_c f_s^2}\right)^2 + 4\pi^2 \left(\frac{EI}{m_c f_s^2}\right)}} \quad (3.135)$$



To determine the conductor stress, the free-span vibration amplitude, which can be calculated with (3.120) is needed. However, its solution provides some difficulties, since this equation contains terms for stochastic wind input energy and conductor damping (and performance with [Stockbridge damper](#)), which cannot be equated mathematically in a simple manner. Hence, vibration amplitudes are approximately determined using the energy balance principle. A stationary vibration condition is assumed for the conductor with free-span amplitude A_f . The vibration modes are assumed as standing harmonic waves, where the exciting frequency complies with Strouhal relation

$$EI \frac{\partial^4 y}{\partial x^4} - S \frac{\partial^2 y}{\partial x^2} + \beta I \frac{\partial^5 y}{\partial x^4 \partial t} + C \frac{\partial y}{\partial t} + \rho A \frac{\partial^2 y}{\partial t^2} = f(x, t) \quad (3.120)$$

$$f_w = \frac{St V_w}{D} \quad (3.136)$$

where f_w is the wind excitation frequency, St the [Strouhal number](#) (between 0.18 and 0.22), V_w the wind velocity and D the conductor diameter.

In a stationary vibration condition, the mean power P_W fed into the system by the wind balances the mean damping power P_S due to the self-damping of conductor and the mean power loss P_D of dampers. These power components depend non-linearly on the free-span amplitude A_f and the excitation or vibration frequency f . In this case, the energy balance is equated as

$$P_W(A_f, f) = P_D(A_f, f) + P_S(A_f, f) \quad (3.137)$$

To determine the free-span amplitude, terms for the quantities P_W , P_D and P_S are required. The expression

$$P_W = f_w^3 D^4 a \cdot g\left(\frac{A_f}{D}\right) \quad g\left(\frac{A_f}{D}\right) = 2.6 \left(\frac{A_f}{D}\right) + 81.2 \left(\frac{A_f}{D}\right)^2 - 76.5 \left(\frac{A_f}{D}\right)^3 \quad P_D = \frac{1}{2} \hat{v}_K^2 Re[Z] \quad P_S = C f_w^p A_f^q H_B \frac{a}{H^r} \quad (3.138)$$

where \hat{v}_K is the velocity amplitude of damper clamps, $Re[Z]$ is the real part of frequency dependent impedance Z of the damper, H is the conductor tensile force, H_B is the conductor minimum failing load. The quantities of damping constant C and exponents p, q, r are determined from measurement at vibrating conductor.

The vibration intensity of a conductor is defined by the free-span vibration angle ψ which results from the free-span amplitude, the vibration frequency and the wavelength.

$$\psi = \frac{2\pi A_f}{\lambda} \quad (3.139)$$

The bending strain of the conductor strands can be taken as a benchmark for their stressing. The relation between the bending strain of a strand ε in the outer layer and the curvature of the conductor is

$$\varepsilon(x) = e w''(x) \quad (3.140)$$

where e is the distance between neutral axis and surface of a strand. For rigidly clamped conductor, the bending strain is obtained using $\omega = 2\pi f_W$ for the resonance condition at the clamping position

$$\varepsilon(0) = e A_f \omega \sqrt{\frac{m_c}{EI}} = e \psi \sqrt{\frac{H}{EI}} \quad (3.141)$$

The conductor bending strain can alternatively be expressed by the bending amplitude w_b . For this purpose, the displacement of the conductor is calculated at a distance x_b from the clamping position. The corresponding bending strain at the clamping position results from

$$\varepsilon(0) = \frac{d w_b \alpha_1}{4} \quad (3.142)$$

$$x_b - \frac{1 - \exp(-\alpha_1 x_b)}{\alpha_1}$$

where d is the diameter of the strand in the outer layer and $\alpha_1 = \sqrt{H/EI}$ with H conductor tensile force and EI the bending stiffness. The correlation between the strain and stress in a strand

$$\sigma = E A_{A1} \quad (3.143)$$

where E_{A1} is the modulus of elasticity.

It is noted that the minimum bending stiffness and maximum bending stiffness of a composite conductor is

$$(EI)_{Min} = \frac{n_{Fe} E_{Fe} \pi d_{Fe}^2 + n_{Ai} E_{Ai} \pi d_{Ai}^2}{64} \quad (EI)_{Max} = \frac{1}{2} \sum_{i=1}^N (I_{pdi} + R_i^2 A_{di}) n_i E_i \quad (3.144)$$

where n = number of strand, N is number of layers counting the core wire as the 1st layer, R_i the average radius of the helix of layer i and I_{pdi} the polar moment of inertia of a strand in layer i :

$$I_{pdi} = \pi d_i^4 / 32 \quad (3.145)$$

For Galloping, which is excited by wind at 6 – 25 m/s with transversal and torsional oscillation, is a flow-induced oscillation. Aerodynamic forces, f_L , and f_D , and moment, M_w , act at the shear center. The initial ice position is θ_{ice} and θ is the actual rotation of the conductor; φ is the angle of attack. The regions where the lift curve derivative crosses the drag curve are regions of possible Den Hartog instability. It is remarkable that a small variation in the ice shape leading to a slightly asymmetric lift curve results in a Den Hartog instability region around -50° but not at $+50^\circ$.

To evaluate possible instabilities, the vertical force acting on the (moving vertically and torsionally) conductor is calculated as follows (noting that α is negative):

$$f_w = f_L \cos \alpha + f_D \sin \alpha \quad (3.146)$$

Instability occurs in a vertical movement if a perturbation in the vertical movement (thus creating a vertical speed) would see a change in applied force which would amplify the movement. For example, a positive vertical speed would generate an increase of vertical net force in the same direction, in other terms:

$$\Delta f_w > 0 \quad \text{unstable} \quad (3.147)$$

To establish the variation of the force, we will make the simplified hypothesis that the drag coefficient is constant and note that the angle α is very small.

$$\Delta f_w = \Delta f_L + f_D \Delta \alpha, \quad \Delta \alpha = -\Delta \dot{y} / U_0$$

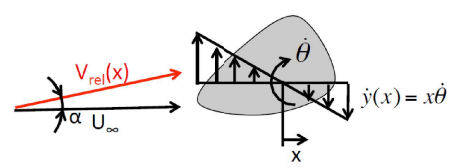
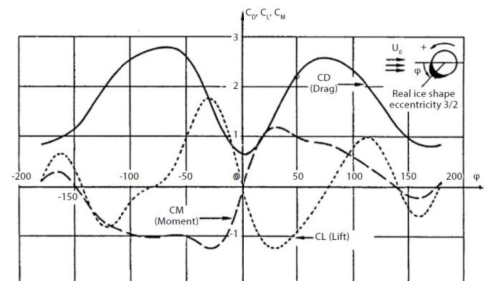
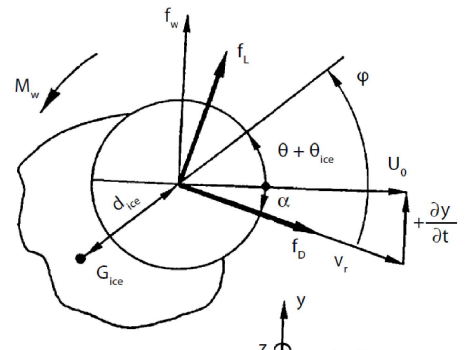
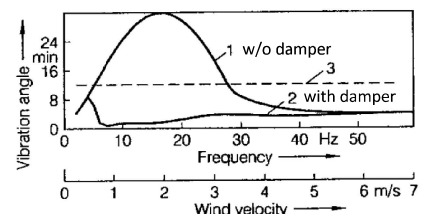
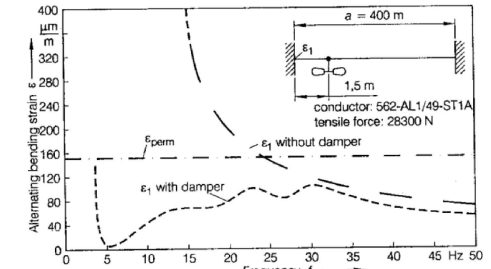
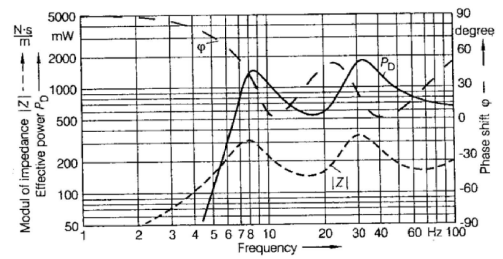
$$\Delta f_L = k_D \frac{\partial C_L}{\partial \varphi} \Delta \varphi = k_D \frac{\partial C_L}{\partial \varphi} (\Delta \theta - \Delta \alpha) \quad (3.148)$$

$$\Delta f_w = k_D \left[C_D \Delta \alpha + \frac{\partial C_L}{\partial \varphi} (\Delta \theta - \Delta \alpha) \right]$$

So that instability criteria are predictable. Note that $\Delta \alpha$ is negative for an upward movement, instability depends on the torsional behavior. Two cases have to be considered.

$$\text{Case 1: No Torsion: } \Delta \theta = 0 \rightarrow C_D - \frac{\partial C_L}{\partial \varphi} < 0 \quad \text{unstable} \quad (3.149)$$

Case 2: With Torsion ($\Delta \theta \neq 0$): These galloping cases are considered as aeroelastic as structural data (like the ratio vertical/torsional frequencies, inertial effect, torsional stiffness, damping) may interact strongly in the phenomenon. Not only aerodynamic properties (= lift, drag and moment aerodynamic curves) are important but also structural data play a major role.



Reference:

- [1] Kiessling F. et al (2003) Overhead Power Lines: Planning, Design, Construction – Chapter 11: Conductor Vibrations, Chapter 12: Support, 13: Foundation, 14: Sag and Tension Calculation
- [2] Brewer A. (2017) Dynamic Wind Load Modelling of High Overhead Transmission Line Towers (Foundation and Dynamics)
- [3] Papailiou K. O. (2017) Overhead Lines – Chapter 5: Structural and Mechanical Design
- [4] CIGRE (2007) Sag-Tension Calculation Methods for Overhead Line (No. 324)
- [5] Matos I.M. (2020) Fretting Fatigue of 6201 Aluminum Alloy Wires of Overhead Conductors
- [6] CIGRE (2012) Mechanical Security of Overhead Lines Containing Cascading Failures and Mitigating Their Effects (No. 515)
- [7] Liu X. (2020) Galloping Stability and Aerodynamic Characteristic of Iced Transmission Line Based on 3-DOF

Chapter 3 - Summary

- 3.1 Sag and Tension**
- Vertical Force & Horizontal Force: $\frac{V}{H} = \frac{dy}{dx}$ Accurate Solution: $\frac{d^2y}{dx^2} = \frac{m_C g}{H} \sqrt{1 + \left(\frac{dy}{dx}\right)^2} \rightarrow y = \frac{H}{m_C g} \cosh \frac{m_C g}{H} x$
- Length: $L = \int_{x_A}^{x_B} \sqrt{1 + \left(\frac{dy}{dx}\right)^2} dx$ Simplified Solution: $\frac{d^2y}{dx^2} = \frac{m_C g}{H} \rightarrow y = \frac{m_C g}{2H} x^2$
- Sag: $f = \frac{h}{a}(x - x_A) + \frac{m_C g}{2H}(x_A^2 - x^2) \rightarrow f_{Max} = \frac{m_C g a^2}{8H}$ Location: $x_A = -\frac{a}{2} + \frac{H - h}{m_C g a}$
- Attachment Tensile Force: $S_A = H + f_e \cdot m_C g, S_B = H + (f_e - h) \cdot m_C g$
- Length inc. Thermal and Elastic Elongation: $L_2 = L_1(1 + \varepsilon_t(T_2 - T_1))(1 + \frac{S_2 - S_1}{EA})$
- Conductor State-Change Equation: $H_2^2[H_2 - H_1 + \frac{EA(a m_{C1} g)^2}{24H_1^2} + EA \varepsilon_t(T_2 - T_1)] = \frac{EA(a m_{C2} g)^2}{24}$
- Ruling Span: $a_{id} = \sqrt{\frac{\sum_{i=1}^n a_i^3}{\sum_{i=1}^n a_i}}$ Slack: $L - a = \left(\frac{2H}{w}\right) \sinh\left(\frac{wa}{2H}\right) - a \approx a^3 \left(\frac{w^2}{24H^2}\right) \approx f_{Max}^2 \left(\frac{8}{3a}\right)$
- Combined Elastic Modulus: $E_{AS} = E_A \frac{A_A}{A_{AS}} + E_S \frac{A_S}{A_{AS}}$ Combined Expansion Coefficient: $\alpha_{AS} = \alpha_A \frac{E_A}{E_{AS}} \frac{A_A}{A_{AS}} + \alpha_S \frac{E_S}{E_{AS}} \frac{A_S}{A_{AS}}$
- 3.2 Structural Analysis for Truss System**
- Total Bracing Force: $D_A = \left(\sum P_b + \Delta \sum P_V b_V + \sum M_T \frac{b_A}{b_B} \right) \frac{l_d}{2b_{Ao} b_{Au}}$

- Finite Element Method: $\begin{pmatrix} \mathbf{F}_a \\ \mathbf{F}_b \end{pmatrix} = \begin{pmatrix} \mathbf{K}_{aa} & \mathbf{K}_{ab} \\ \mathbf{K}_{ba} & \mathbf{K}_{bb} \end{pmatrix} \begin{pmatrix} \mathbf{U}_a \\ \mathbf{U}_b \end{pmatrix} \rightarrow \mathbf{U}_a = \mathbf{K}_{aa}^{-1} (\mathbf{F}_a - \mathbf{K}_{ab} \mathbf{U}_b)$
- 3.4 Fatigue Model**
- Basquin's Law: $N_f = N_0 \left(\frac{S}{S_0} \right)^{\frac{1}{b}}$ Goodman's Law: $\left(\frac{\sigma_a}{\sigma'_a} \right) + \left(\frac{\sigma_m}{\sigma_u} \right) = 1 \rightarrow \sigma'_a = \frac{\sigma_a}{1 - \frac{\sigma_m}{\sigma_u}}$
- Basquin-Goodman-Manson's Law: $\frac{\Delta \varepsilon}{2} = \frac{\sigma_f}{E} (2N_f)^b + \varepsilon_f (2N_f)^c$
- Smith-Topper-Watson: $\sigma_{max} \varepsilon_a = \frac{(\sigma_f')^2}{E} (2N_f)^{2b} + \sigma_f' \varepsilon_f (2N_f)^{b+c}$ Neuber Correction: $E\varepsilon = \sigma / \sqrt{1 - \left(\frac{\sigma}{\sigma^*} \right)^2}$

- 3.6 Dynamic Modelling**
- Second Order Forced Vibration: $\ddot{u} + 2\zeta\omega_0\dot{u} + \omega_0^2 u = f_0 \sin(\omega t) \rightarrow X_0 = H(\omega)f_0 = \frac{f_0}{\omega_0^2 - \omega^2 + j2\zeta\omega_0\omega}$
- with amplitude and angle: $|H(\omega)| = \frac{1}{\sqrt{(\omega_0^2 - \omega^2)^2 - (2\zeta\omega_0\omega)^2}}, \angle H(\omega) = \tan^{-1} \left(\frac{2\zeta\omega_0\omega}{\omega_0^2 - \omega^2} \right)$
- With infinitesimal small pulse load: $du(t_c) = e^{-\zeta\omega_0(t_c-\tau)} \left(\frac{f(\tau)d\tau}{m\omega_d} \sin \omega_d(t_c - \tau) \right)$

- It results in Duhamel Integral: $u(t_c) = \frac{1}{m\omega_d} \int_0^t e^{-\zeta\omega_0(t-\tau)} f(\tau) \sin \omega_d(t - \tau) d\tau$
- 3.7 Elastic Model**
- Elastic Model: $EI \frac{\partial^4 \omega}{\partial x^4} - H \frac{\partial^2 \omega}{\partial x^2} + m_C \frac{\partial^2 \omega}{\partial t^2} = q_W(x, t) + q_D(\omega, \dot{\omega}, t)$ Strouhal Number: $f_W = \frac{St V_W}{D}$
- Natural Frequency: $f_s = \frac{k}{2a} \sqrt{\frac{H}{m_C} \sqrt{1 + \frac{(k\pi a)^2 EI}{H}}} \quad \left(f = \frac{k}{2a} \sqrt{\frac{H}{m_C}} \right)$ Den Hartog Instability: $\Delta\theta = 0 \rightarrow C_D - \frac{\partial C_L}{\partial \phi} < 0 \quad \text{unstable}$
- Stiffness: $c = \sqrt{\frac{H}{m_C}} \left(c_s = \sqrt{\frac{H}{m_C} \sqrt{1 + \frac{(k\pi a)^2 EI}{H}}} \right)$
- Wavelength: $\lambda_s = \sqrt{\frac{H}{2m_C f_s^2} + \sqrt{\left(\frac{H}{2m_C f_s^2} \right)^2 + 4\pi^2 \left(\frac{EI}{m_C f_s^2} \right)}} \quad \left(\lambda = \frac{1}{f} \sqrt{\frac{H}{m_C}} \right)$

THE END